



HAL
open science

Oxytocin modulates the neurocomputational mechanisms engaged in learning social hierarchy Authors

Jiawei Liu, Chen Qu, Rémi Phillipe, Siying Li, Edmund Derrington, Brice Corgnet, Jean-Claude Dreher

► **To cite this version:**

Jiawei Liu, Chen Qu, Rémi Phillipe, Siying Li, Edmund Derrington, et al.. Oxytocin modulates the neurocomputational mechanisms engaged in learning social hierarchy Authors. 2024. ⟨hal-04297163⟩

HAL Id: hal-04297163

<https://hal.science/hal-04297163v1>

Preprint submitted on 21 Nov 2023

HAL is a multi-disciplinary open access archive for the deposit and dissemination of scientific research documents, whether they are published or not. The documents may come from teaching and research institutions in France or abroad, or from public or private research centers.

L'archive ouverte pluridisciplinaire **HAL**, est destinée au dépôt et à la diffusion de documents scientifiques de niveau recherche, publiés ou non, émanant des établissements d'enseignement et de recherche français ou étrangers, des laboratoires publics ou privés.



HAL Authorization

Oxytocin modulates the neurocomputational mechanisms engaged in learning social hierarchy

Authors

Jiawei Liu^{1,2,3†}, Chen Qu^{3†}, Rémi Phillippe^{1,2}, Siying Li^{3,4}, Edmund Derrington^{1,2}, Brice Corgnet⁵, Jean-Claude Dreher^{1,2*}

¹ Laboratory of Neuroeconomics, Institut des Sciences Cognitives Marc Jeannerod, CNRS, Lyon, France.

² Université Claude Bernard Lyon 1, Lyon, France.

³ Key Laboratory of Brain, Cognition and Education Sciences, Ministry of Education, China; School of Psychology, Center for Studies of Psychological Application, and Guangdong Key Laboratory of Mental Health and Cognitive Science, South China Normal University, China.

⁴ Faculty of Education, Northeast Normal University, Changchun, China.

⁵ EM Lyon Business School, and CNRS, GATE Lab, UMR 5824, Ecully, 69130, France.

† These authors contributed equally to this work.

* Lead contact, Correspondence: dreherjeanclaude@gmail.com

Abstract

It is unknown whether oxytocin modulates the neurocomputational mechanisms engaged in learning social ranks and in making transitive inferences based on social memory. In a new fMRI study combined with computational modeling, participants learned two non-linear social hierarchies by trial and error, one in which they were embedded and the other not. During a subsequent test phase, they inferred hierarchical relationships between face pairs never encountered during training. During training, oxytocin modulated computations of the action selection policy from a Reinforcement Learning-ELO model and this effect was associated with increased activity of the medial prefrontal cortex. During test phase, oxytocin modulated the balance between self-other social memory, boosting correct performance for the other-related hierarchy and increasing amygdala response. These findings demonstrate that oxytocin modulates the brain computations underlying both choice selection related to social ranks and social memory needed to make transitive inferences.

34 **Highlight sentences**

- 35 ● Oxytocin modulates brain computations underlying choice selection of social ranks
- 36 ● OXT increases the activity of the ventromedial prefrontal cortex and the posterior
37 cingulate cortex, which compute the action selection policy at the time of choice.
- 38 ● OXT modulates the memory of social hierarchies differently depending on whether one
39 is embedded in the hierarchy or not.
- 40 ● This effect occurs both the behavioral and the brain system levels in the amygdala and
41 parahippocampal regions

42 **Keywords**

43 Reinforcement learning; model-based fMRI; Social hierarchy; Self-other distinction;
44 Oxytocin.
45

46 **1. Introduction**

47 Dominance hierarchies, characterized by ranking systems based on the relative social
48 power of individuals within a group, are a major evolutionary force that drive dyadic
49 asymmetries. Dominance hierarchies may be learned incrementally, by accumulating
50 feedback on relationships to specific members of a social group. The learning of
51 hierarchical status can be framed as a reinforcement learning (RL) problem, inspired by
52 neurocomputational approaches traditionally applied to non-social cognition, both when
53 learning dominance relationships by observation of other interacting individuals (Kumaran
54 et al., 2016), or by direct dyadic competitive interactions between oneself and another
55 individual (Ligneul et al., 2016; Qu et al., 2017). The medial prefrontal cortex (mPFC) and
56 the amygdala/hippocampus may play distinct computational roles during and after
57 learning ‘linear’ ($r_1 < r_2 < \dots < r_k$) social hierarchies. During learning, the mPFC (both dorsal
58 and ventral parts) has been shown to compute the monitoring and updating of dominance
59 status. These are fundamental signals needed to make choices between two individuals
60 when learning their social dominance relationship by trial and error (Janet et al., 2022;
61 Kumaran et al., 2016; Ligneul et al., 2016). In contrast, when required to infer the
62 relationship between two non-adjacent members in a linear hierarchy, while only adjacent
63 relationships have been learned, the amygdala-hippocampal complex is necessary to
64 retrieve learned relationships between other members of the social structure from social
65 memory (Kumaran et al., 2012, 2016).
66

67 Previous studies have considered social hierarchies as a series of relationships whereby
68 individuals are ranked successively in a linear fashion (Jensen et al., 2019; Kumaran et al.,
69 2012, 2016). However, social hierarchy in real life is often not a simple linear structure.
70 Real hierarchies often include individuals of equal social ranks. The first question we
71 addressed is how such non-linear ‘diamond-shaped’ hierarchies might be learned and
72 represented in the brain (Fig. 1). We characterize the computations and brain systems
73 engaged when making transitive inferences, after learning a diamond-shaped hierarchy by
74 repeated learning trials between pairs of people with feedback. These transitive inferences
75 were performed in the absence of corrective feedback, while participants viewed pairs not
76 encountered during training. Such transitive inferences require social memory of the
77 previously learned paired members, to infer the relative ranks of members, based on
78 partial information provided during the learning trials.

79 Oxytocin (OXT) is an evolutionarily conserved neurohypophysial hormone, engaged in
80 lactation and parenting. The function of this hormone might have been sculpted during
81 evolution to facilitate the expression of adaptive social behaviors, as required for forming
82 hierarchical relationships (Lee et al., 2019). There is evidence in non-human primates and
83 rodents that OXT modulates social hierarchy. For example, OXT suppresses vigilance
84 towards faces of dominant males in the rhesus macaque (Chang & Platt, 2014; Ebitz et al.,
85 2013) and relaxes social interactions between monkeys, thereby flattening the social
86 hierarchy (Jiang & Platt, 2018). In mice, socially dominant males have higher OXT
87 receptor binding compared to subordinates, in brain regions such as the amygdala (Lee et
88 al., 2019). This effect may reflect that the different social environments experienced by
89 dominant and subordinate animals may alter receptor expression, and potentially facilitate
90 adaptive social behaviors.

91 Here, we focused on the neurocomputational processes that take place while learning non-
92 linear (diamond-shaped) social hierarchies by observation. We used model-based
93 functional magnetic resonance imaging (fMRI), and an extension of a two-phase social
94 hierarchy learning paradigm. Participants learned hierarchical ranks by trial and error
95 during a training phase (Fig. 1). Then, during a test phase, they made transitive inferences
96 of relative hierarchical rank between pairs of individuals who were never encountered
97 before. We developed a new reinforcement learning model to account for social hierarchy

98 learning when it is necessary to learn both equal ranks and different ranks and investigated
99 how OXT administration might impinge on the model parameters.

100 We tested whether OXT plays a specific role in either phase of our new social hierarchy
101 learning paradigm while: (a) learning social ranks by reinforcement during the training
102 phase and (b) encoding and retrieval of social memories, required to make transitive
103 inferences between learned members of the hierarchical structure during the test phase.
104 We also compared how OXT administration might affect these processes with respect to
105 self- and other-orientated hierarchies (i.e., when oneself is included or not in the
106 hierarchy) (Fig. 1C).

107 During training, we hypothesized that learning non-linear social hierarchies engaged
108 computational mechanisms and brain representations similar to those engaged in learning
109 one-dimensional linear social hierarchies by observation. Specifically, we hypothesized
110 that the mPFC, engaged in learning linear social hierarchy (Janet et al., 2022; Kumaran et
111 al., 2016; Ligneul et al., 2016), will also be engaged when learning diamond-shaped social
112 hierarchies. Preliminary evidence suggests that OXT may modulate distinct
113 neurocomputational mechanisms engaged in reinforcement learning, including selection
114 between different options during choice behavior (Piva & Chang, 2018) or prediction
115 error, as previously suggested in the domain of prosocial behavior (Clark-Elford et al.,
116 2014; Hu et al., 2015; Hung et al., 2017; Hurlemann et al., 2010; Ide et al., 2018; Kruppa
117 et al., 2019; Liao et al., 2020; Martins et al., 2022; Zhuang et al., 2021). Therefore, we
118 hypothesized that OXT could modulate both action selection policy, reflecting the
119 probability of choosing the correct rank of a given individual and updating of social ranks
120 at the time of outcome.

121 During the test phase of the task, social memory processes are engaged when making
122 transitive inferences between members of the learned structure (pairs of individuals who
123 were never encountered together before). Previous studies in mice indicate that OXT
124 regulates social memory (Baram et al., 2021; Ferguson et al., 2000; H. J. Lee et al., 2008;
125 MacBeth et al., 2009; Raam et al., 2017; Wirth et al., 2021). We thus hypothesized that
126 OXT affects social memory also in humans and could modulate responses of the
127 amygdala/hippocampal region, which are known to be engaged when making transitive
128 inferences between items (Kumaran et al., 2016). Finally, we tested whether OXT

129 modulates social memory and its neural correlates differently for social hierarchy
130 structures in which participants were embedded or not (Self vs Other-orientated
131 hierarchy). This is because well-functioning social interactions may require differential
132 other-related and self-related information processing (Bang et al., 2022; Ereira et al.,
133 2020; Wittmann et al., 2016) and because OXT differently modulates value computation
134 of self–other allocations (Chang, Barter, et al., 2012; Chang & Platt, 2014; Liao et al.,
135 2020) and in-group/out-group decisions (De Dreu et al., 2010).

137 2. Results

138 2.1 Behavioral results

139 We fitted two generalized linear mixed-effects models (GLMM) to analyze how
140 performance of learning social ranks during the training phase (GLMM1) or making
141 transitive inferences during the test phase (GLMM2) varied according to the Status of the
142 members (Superior, Intermediate and Inferior), Hierarchy Orientation (Self: participant at
143 the center of the hierarchy, labelled ‘Self’ *versus* Other: another participant at the center of
144 the hierarchy, labelled ‘Other’), 9 Blocks, Group (Oxytocin *versus* Placebo) and pertinent
145 interaction factors.

146 During the training trials, participants performed better on trials comparing hierarchy
147 members with Superior (odds ratio = 3.392, $p < 0.001$) and Inferior (odds ratio = 3.156, p
148 < 0.001) status, compared to trials involving hierarchy members of equal status (Fig. 2A).
149 A *post-hoc* test showed that participants also performed better on trials involving Superior
150 than Inferior hierarchy members (odds ratio = 1.331, SE = 0.06, $p < 0.001$, $z = 6.316$). As
151 the number of blocks increased, participants improved their performance (odds ratio =
152 1.433, $p < 0.001$). An interaction effect of Group \times Block further showed that participants
153 in the Placebo group were more likely than those in the Oxytocin group to improve
154 performance over consecutive blocks (odds ratio = 0.966, $p = 0.042$, Fig. 2B). We also
155 found participants learned better in the Self- than Other-orientated hierarchy (odds ratio =
156 1.237, $p < 0.001$, Fig. 2C). There was a significant interaction effect of Hierarchy
157 Orientation (Self/Other) \times Status (Superior: odds ratio = 0.543, $p < 0.001$; Inferior: odds
158 ratio = 0.616, $p < 0.001$). A *post-hoc* test revealed that participants performed better in

159 Self-orientated Hierarchy than the Other-orientated Hierarchy condition only for trials
160 involving Intermediate status (odds ratio = 1.783, SE = 0.183, $p < 0.001$, $z = 5.646$). With
161 regard to results of response time (RT) analyzed by LMM1 during the training trials, RTs
162 were longer for trials involving both Superior ($b = 0.032$, $p = 0.008$) and Inferior ($b =$
163 0.128 , $p < 0.001$) hierarchy elements than trials involving the elements of Intermediate
164 status (Fig. 2A, right). A *post-hoc* test further revealed that RTs was shorter for trials
165 involving Superior elements than Inferior ($b = -0.096$, SE = 0.009, $p < 0.001$, $z = -10.529$).
166 These results indicate that participants' RTs are consistent with a speed-accuracy tradeoff.
167 Moreover, RTs gradually reduced over consecutive trial blocks, indicating faster
168 responses as the hierarchies were learned better ($b = -0.045$, $p < 0.001$, Fig. S1A). The
169 Oxytocin group also showed quicker reduction of RTs than the Placebo group over blocks
170 ($b = -0.022$, $p < 0.001$, Fig. S1A). In addition, RTs reduction across blocks was faster in
171 the Self than the Other-orientated condition ($b = -0.007$, $p = 0.034$, Fig. S1B), suggesting
172 people learn faster when they are included in the hierarchy.

173 In test trials, participants improved performance over consecutive blocks (GLMM2, odds
174 ratio = 1.373, $p < 0.001$). The Oxytocin group improved accuracy faster across blocks than
175 the Placebo group (odds ratio = 1.04, $p = 0.023$, Fig. 2D). The interaction effect of Group
176 \times Hierarchy Orientation showed that the Oxytocin group outperformed the Placebo group
177 in the Self-orientated hierarchy compared to Other-orientated hierarchy (odds ratio =
178 1.262, $p = 0.005$, Fig. 2E). Analysis of RT by LMM2 revealed that participants were
179 slower in the Self-orientated hierarchy condition compared to Other-orientated hierarchy
180 ($b = 0.09$, $p < 0.001$). Moreover, participants decreased their RT faster across blocks in the
181 Self-orientated hierarchy compared to the Other-orientated condition ($b = -0.014$, $p <$
182 0.001). The Oxytocin group also decreased RT faster over blocks than the Placebo group
183 ($b = -0.015$, $p < 0.001$). See supplementary Table S1 & S2 for complete behavioral results.

184 2.2 Computational model results

185 We tested 5 models accounting for how learning the item values in the hierarchy structure.
186 Model 1 was the RL-ELO model (Model 1) which has been shown to be successful to
187 account for learning linear hierarchies (Kumaran et al., 2016). Model 2 was a modified
188 RL-ELO model with two different learning rates for hierarchically superior and inferior
189 members of the hierarchy. Model 3 was the classical Rescorla-Wagner (RW) model and

190 model 4 was the Value Transfer model, which are known to fail in learning linear
191 hierarchies as they associate equally with positive and negative outcomes (Kumaran et al.,
192 2016). We also developed a new RL-ELO model, called the Combined RL-ELO-based
193 associative learning model (Model 5), which enables to learn hierarchical structures
194 involving equal ranks (i.e., non-linear 'diamond shape'). Because learning equal ranks
195 may involve different strategies than learning unequal ranks, we assumed that learning
196 equal ranks was equivalent to memorizing matching pairs. For this reason, we propose a
197 model in which learning occurs in two steps. First, an associative learning rule is updated
198 according to the fact that ranks are equal or unequal. Second, the value of each item in the
199 presented pair is updated according to the past choice and reward. That is, if ranks
200 between items are unequal, the value of the highest (or the lowest) item in the hierarchy is
201 increased (or decreased respectively). If items in the pair were equal, their values became
202 closer according to a proportion of their initial distance (See also computational modeling
203 section in methods). All models were fitted separately for choices by each individual using
204 Matlab VBA-toolbox (Daunizeau et al., 2014). Protected exceedance probability (PXP)
205 was used for model selection. It accounts for the probability that the considered model is
206 more frequent in the studied population, which can be used as a quantitative measure of
207 the amount of evidence for the best model (Daunizeau et al., 2014). The Self- and the
208 Other-orientated conditions were fitted separately to allow participants to learn differently
209 between conditions.

210 Comparisons between models showed that the best model was the RL-ELO-based
211 associative learning model (Model 5: PXP = 1; Fig. 3D), with a single alpha learning rate
212 to update item values for each of the two hierarchy orientations (Self and Other). The fit of
213 this model with the performance results are plotted over blocks for correctly selected items
214 during training (Fig. 3A) and test blocks (Fig. 3B). The mean evolution of each item
215 power ($Q_{(i)}$) across all subjects is shown in Fig. 3C. Finally, we ran a 2-way mixed
216 ANOVA analysis on the parameters of the RL-ELO-based associative learning model
217 according to hierarchy orientation (Self/Other: within-subject factor) and treatment group
218 (Oxytocin/Placebo: between-subject factor) (See supplementary Table S7). We observed
219 significant effects only for the learning rate α_{eq} used to update choices of members of
220 equal rank. That is, for this learning rate α_{eq} , we observed a main effect of hierarchy
221 orientation ($F_{(1,56)} = 7.42, p = 0.009, \eta^2 = 0.04$; Self: $\text{Mean}(\alpha_{eq}) = 0.10$, Other: $\text{Mean}(\alpha_{eq}) =$

0.18; Fig. 3E) and a marginally significant Group effect ($F_{(1,56)} = 3.53, p = 0.065, \eta^2 = 0.003$; OXT: $\text{Mean}(\alpha_{eq}) = 0.10$, Placebo: $\text{Mean}(\alpha_{eq}) = 0.18$), but no interaction effect ($F_{(1,56)} = 0.02, p = 0.89, \eta^2 = 0.001$).

2.3 Brain regions engaged in learning social hierarchy

As the Combined RL-ELO-based associative learning model can predict the participants' behavior during social hierarchy learning, we fitted parametric trial-by-trial regressors of the model-estimated probability that a participant chooses the correct response as a proxy of the knowledge of the hierarchical structure (GLM1). This probability of choosing the correct answer was added as a parametric regressor at the time of presentation of the two faces. When collapsing over the Placebo and Oxytocin groups, a whole brain analysis indicated that the ventromedial prefrontal cortex (vmPFC), posterior cingulate cortex (PCC) as well as the temporal gyrus, parietal lobule and occipital cortex encoded the probability of choosing the correct answer during training (Fig. 4A; also see Supplementary Table S4 for details of activated regions). Subsequently, we carried out region-of-interest (ROI) analyses in vmPFC and PCC, based on independent coordinates from a meta-analysis related to social learning and self-referential processing (Bartra et al., 2013). Beta estimate values were extracted from the interaction between hierarchical orientation (Self/Others) and Group treatment during the learning trials, and a follow-up mixed ANOVA was performed. Results showed a significantly stronger neural response in the Oxytocin than the Placebo group in both ROIs (vmPFC: $F_{(1,56)} = 4.06, p = 0.0488, \eta^2 = 0.033$, Fig. 4B; PCC: $F_{(1,56)} = 4.66, p = 0.035, \eta^2 = 0.023$, Fig. 4C).

In addition, the prediction error (PE), which reflects the difference between expected and actual rewards, was encoded at the outcome feedback in training trials by robust activity in the vmPFC and the ventral putamen bilaterally (GLM2, Fig. 5A). However, none of these regions showed significant differences between Oxytocin and the Placebo groups (illustrated in Fig. 5B, 5C & 5D).

2.4 Brain regions engaged in social memory when making transitive inferences

During the test phase, a whole brain fMRI data analysis (GLM3, using the probability of choosing the correct response computed by the RL-ELO associative model) showed

252 engagement of a brain network including the mPFC, the anterior and posterior cingulate
253 cortex and the temporal cortex (Fig. 6A). Moreover, comparison in the test phase between
254 hierarchy orientation (Other > Self) revealed stronger activity in the dorsal anterior
255 cingulate cortex (dACC, Fig. 6B & 6C), the right inferior parietal lobule (IPL) and in the
256 precentral gyrus. We also examined putative differences between groups in vmPFC and
257 PCC ROIs. However, no significant difference between placebo and Oxytocin groups
258 were observed (vmPFC: $t = 2$, $df = 56$, $p = 0.1$; PCC: $t = -1$, $df = 56$, $p = 0.3$).

259 Finally, because the behavioral analyses indicated an interaction effect between Group and
260 Hierarchy Orientation during the test phase (Fig. 2E), we investigated the brain correlates
261 of this behavioral effect (GLM4). This analysis revealed an interaction with the same
262 pattern between Group and Hierarchy Orientation (Fig. 7A), observed in the left amygdala
263 (Fig. 7B) and in the right parahippocampal region (Fig. 7C). BOLD response in these
264 regions was stronger during the Self- than Other-orientated hierarchy trials in the Placebo
265 group, whereas in the Oxytocin group activity was stronger for the Other- than for the
266 Self-orientated hierarchy.

267 3. Discussion

268 The present study investigated how intranasal OXT modulates the neurocomputational
269 mechanisms subserving learning and remembering diamond-shaped social hierarchies in
270 which participants were or not embedded. Our results provide mechanistic insights into
271 how OXT modulates the neurocomputational signals determining action selection policy
272 during learning and social memory recall when making transitive inferences in the test
273 phase. OXT increased activity of the vmPFC and PCC related to action selection policy,
274 reflecting the probability of identifying the correct rank relationship between two
275 individuals (i.e., equal or unequal ranks in the non-linear ‘diamond shape’ structure).
276 During the test phase, participants had to decide, by making transitive inferences, whether
277 two items were of equal or unequal ranks. In this test phase, OXT led to improved
278 performance for the Other-orientated hierarchy, and reduced performance for the Self-
279 orientated hierarchy. This interaction between group (OXT, Placebo) and Self/Other-
280 hierarchy orientation was associated with higher activity in the amygdala and the
281 parahippocampal region. Together, these findings characterize how OXT modulates

282 neurocomputational signals engaged in learning social hierarchies and in remembering
283 learned social relationships.

284 Social dominance hierarchies are a common form of social organization that requires
285 individuals to learn and remember their status relative to others. Once relative status in a
286 given structure has been learned, individuals maintain consistent patterns of social
287 behavior (e.g. competitive or submissive) based on their past social interactions (Chase &
288 Seitz, 2011; Williamson et al., 2016). Unlike previous studies on linear social hierarchy
289 structure (Kumaran et al., 2012; Vasconcelos, 2008), we developed a diamond-shaped
290 social hierarchy task in which relative ranks could be equal. Our combined RL-ELO-based
291 associative learning model captured the learning of such hierarchies. This model considers
292 learning social hierarchy as an incremental process accumulating feedback concerning
293 members of the social group, in which one may or may not be embedded. Our RL-ELO-
294 based model reflects dynamic learning of social relationships. This was done in a two-
295 stage process. Participants updated the associative value representing the learned
296 association between the pairs and the action of choosing equality between members, given
297 past exposure to this pair. Then, participants updated their representations of the hierarchy
298 structure by correcting the value of each item of the pair according to past choices and
299 rewards. This model allowed us to identify the medial PFC and PCC as implementing the
300 action selection policy. Moreover, the PE engaged the ventral putamen and the vmPFC
301 during the feedback outcome, extending the classical PE signal to learning of social
302 relationships (30, 38, 39). Recent computational models and experimental studies have
303 proposed that the same brain representations that map space can be extended to a broad
304 range of non-spatial problems in abstract cognitive space (Kurth-Nelson et al., 2015).
305 These studies support that the mPFC and the hippocampus are involved in non-spatial
306 relational memory tasks, allowing them to make transitive inferences (Boorman et al.,
307 2021; Dayan, 1993; Sharpe et al., 2017) and to organize the relationships between entities
308 (e.g., places, objects, people, events, or abstract task states) to afford generalization and
309 flexible decision making. Our results extend these findings and explain how abstract
310 structural relationships such diamond-shaped social hierarchies are learned at the
311 computational level.

312 Here, we characterize the effect of OXT in dynamic learning of social hierarchy at the
313 neurocomputational level. Our findings demonstrate distinct computational roles of OXT
314 during the training and test phases of the task. During training, OXT modulates the

315 neurocomputational signals needed for implementing an action policy to choose the
316 correct answer. OXT did not modulate learning rate *per se*, nor PE-related brain activity,
317 but modulated the brain regions computing a choice policy during training. There is mixed
318 evidence for a role of OXT on reinforcement learning in humans. Some studies report that
319 OXT may facilitate reinforcement learning (Hu et al., 2015; Hurlemann et al., 2010;
320 Zhuang et al., 2021) and modulate computational signals underlying prosocial
321 reinforcement learning (Martins et al., 2022). However, other studies report that OXT
322 reduces the encoding of PE during in an iterative trust game (Ide et al., 2018) and during
323 social reward learning tasks (Clark-Elford et al., 2014; Kruppa et al., 2019). These mixed
324 findings are consistent with the fact that the social effects of OXT are highly dependent on
325 the behavioral context (Bartz et al., 2011).

326 It has been difficult to separate learning from choice selection processes because value
327 representations drive choosing, as expected values of different available options are
328 compared, and the best is selected. However, they also drive learning, as the expected
329 value of an outcome is compared to the reward that is actually received, and future
330 expectations are updated. Yet, value-based learning and value-based choosing may depend
331 on separate neural representations (Miller et al., 2022; Rudebeck et al., 2017). Our
332 findings demonstrate that OXT modulated the neurocomputational signals engaged in
333 choice selection, increasing engagement of the vmPFC and PCC that encode the action
334 selection policy during learning of the social hierarchy. At the computational level, these
335 results validate the proposal that OXT may modulate the option selection stage, shifting
336 the choice probability curve (Piva & Chang, 2018), and increasing sensitivity to the
337 relative value during a two-choice economic task (Chang et al., 2011; Piva et al., 2017).

338 During the test phase, OXT differentially modulated social memory needed for transitive
339 inferences according to whether the participant was embedded or not in the hierarchy.
340 Thus, OXT enhanced performance for the making of transitive inferences with respect to
341 the other-related hierarchy, and reduced performance for the hierarchy in which the
342 participant themselves was embedded. At the brain system level, OXT modulated amygdala
343 and parahippocampal activities when making transitive inferences. These brain regions
344 showed interactions in the same direction between group treatment and hierarchy
345 orientation factors. The amygdala and parahippocampal regions have previously been
346 found to encode the status of individuals in linear hierarchies (Kumaran et al., 2016). Both
347 of these regions are rich in OXT receptors and receive OXT from the axonal projections of

348 parvocellular neurons in the hypothalamus (Hawthorn et al., 1985; Jurek & Neumann,
349 2018; Thijssen & Wiegerink, 1978). Thus, they are in a critical position to be regulated by
350 OXT. The amygdala directly mediates OXT influences on social behavior in rodents
351 (Ferguson et al., 2001; Huber et al., 2005) and non-human primates (Chang et al., 2015).
352 OXT regulates social memory inferences in rodents and non-human primates (Ferguson et
353 al., 2000; H. J. Lee et al., 2008; MacBeth et al., 2009). For example, OXT receptors are
354 causally involved in social memory in rodents. Knockout of the OXT gene results in the
355 failure of male mice to develop social memory but treatment with OXT rescued this
356 (Ferguson et al., 2000). In rhesus macaques, OXT delivered directly into the basolateral
357 amygdala enhances prosocial tendencies and attention to the recipients of prosocial
358 decisions (Chang et al., 2015). Moreover, OXT modulates value computation of self–other
359 allocations, amplifying both vicarious reinforcement and self-reinforcement in rhesus
360 macaques (Chang, Barter, et al., 2012; Chang & Platt, 2013)). In humans, OXT influences
361 the balance between self and other mental processes (e.g., trust and prosocial behavior)
362 and their underlying neural mechanisms (De Dreu, 2012; Feng et al., 2020; Liao et al.,
363 2020; Tomova et al., 2019; Zhao et al., 2016). Together, these studies provide behavioral
364 and neuroscientific evidence for OXT effects on self-other referential processing. Our
365 findings extend these previous studies in an important way to self-other social memory
366 when making transitive inferences. They indicate distinct patterns of OXT modulation of
367 brain activities engaged in social memory, when one is oneself (or not) embedded in the
368 hierarchy. Overall, our findings show that the effects of OXT on social memory are
369 modulated by self-other regarding considerations, and that these effects are mediated in
370 the amygdalo-hippocampal complex.

371 We also observed a modulation for Other- vs Self-orientated hierarchy in the dACC,
372 related to action selection policy during the test phase (Fig. 6). This brain region was more
373 robustly engaged for Other- than Self-orientated social hierarchy during the test trials.
374 Efficient social interactions require processing of both Other-related and Self-related
375 information (Bang et al., 2022; Ereira et al., 2020; Wittmann et al., 2016). The anterior
376 cingulate gyrus (ACCg) is implicated in empathy, social learning (Camille et al., 2011;
377 Hadland et al., 2003; Hayden & Platt, 2010), and computations of ‘other-orientated’
378 information (Apps & Ramnani, 2014; Behrens et al., 2008; Chang, Gariépy, et al., 2012).
379 Both the anterior and posterior portions of the ACCg, which overlap with the mPFC and
380 dACC regions in our study, play a key role in facilitating cooperative and competitive

381 interactions, by tracking parameters such as the value and cost of options to others (Apps
382 et al., 2016). As such, our results suggest that the ACCg/mPFC tracks the motivation of
383 others through representations that not only code for the values and costs of reward to
384 other individuals (Apps et al., 2016), but also incorporates status information, particularly
385 within one's own social group.

387 **Limitations and clinical implications**

388 One strength of our study is that we controlled for participants' age and gender (Meyer-
389 Lindenberg et al., 2011; Wang et al., 2017). We decided to test only male participants
390 because the effects of OXT on the brain valuation system are likely to be different in men
391 and women, as OXT increases activation in the ventral striatum in men, but decreases
392 activation in the same region in women during the canonical prisoner's dilemma game
393 (Feng et al., 2015). Another reason for testing only men is that the hierarchy was
394 composed only of male faces, and that men's and women's attitudes towards male faces
395 may differ when learning hierarchies. Further studies will be needed to determine whether
396 the current findings depend upon sex, by comparing hierarchies of women only or mixed
397 samples.

398 Intranasal OXT spray in humans increases OXT levels in the cerebrospinal fluid. The
399 pathways through which OXT reaches the brain include direct nose-to-brain transport,
400 blood-to-brain transport through the blood-brain barrier or a combination of both. A recent
401 study in primates showed that when administered intranasally, OXT can reach the brain
402 (Lee et al., 2020). However, it is also possible that absorption of OXT into the blood
403 might impact the brain indirectly. For instance, peripheral administration of OXT in rats
404 requires vagal signaling to reduce methamphetamine self-administration and reinstatement
405 of methamphetamine-seeking behaviors (Everett et al., 2020). Therefore, we cannot
406 exclude that our behavioral and neural findings of intranasal OXT on option selection
407 during the training stage and on self-other social memory during the test phase, might
408 reflect indirect peripheral effects or a possible interaction between peripheral and central
409 actions. Future studies with concomitant administration of non-brain penetrant antagonists
410 will help to dissect these effects further.

411 Our findings may have clinical implications because OXT may increase social functioning
412 in clinical populations, by modulating the option selection stage of social decision making

413 and/or social memory. Although there have been mixed findings (Cid-jofr et al., 2021;
414 Wang et al., 2017), recent reports have suggested a potential role of OXT to enhance
415 social learning in autism spectrum disorder (ASD) (Kruppa et al., 2019). Single-dose
416 administration studies have generally shown positive effects in ASD (Domes et al., 2013;
417 Gordon et al., 2013), which might be related to an overall enhancement of the
418 motivational system in social contexts. However, longer-term treatment studies, using
419 multiple doses per day, often failed to demonstrate treatment effects (Guastella & Hickie,
420 2016). One reason might be that these were not designed to provide specific social
421 learning contexts around the times of administration (Aoki et al., 2014), or may have
422 interfered with psychotropic medication (Yatawara et al., 2015). Future studies performed
423 in ASD are needed to investigate how OXT modulates social learning and social memory.
424

425 **4. Materials and Methods**

426 **4.1 Participants**

427 We recruited 60 healthy male undergraduate or graduate students (mean age 21.1 years,
428 SD = 2.10, range 18-29 years). Participants were not taking any prescribed drugs and had
429 no history of drug abuse or smoking. We instructed participants to abstain from alcohol
430 and heavy exercise for 24 hours and from food or any beverage other than water for at
431 least 2 hours before scanning. Participants gave written informed consent. Human
432 Research Ethics Committee for Non-Clinical Faculties in South China Normal University
433 approved the study. Two subjects were excluded because of too low performance in the
434 last session (blocks 7~9) both in training and test trials, based on the scale Z-score
435 method, with z scores lower than -2.0, as there was less than a 2.27% probability that
436 these two participants would have a lower average accuracy than our sample. Also, we
437 went through all participants' decisions and found the learning rates of these two
438 fluctuated irregularly. Finally, we included 29 subjects (mean age 20.72 years, SD = 1.87)
439 in the OXT group and 29 subjects (mean age 21.41 years, SD = 2.23) in the Placebo group
440 for analysis.

441 **4.2 Stimulus and Task**

443 The two diamond-shaped hierarchy structures consisted of 16 face pictures (8 for Self-
444 orientated condition, 8 for Other-orientated condition) and two shaded pictures referring to
445 Self and Other (letter 'X' as its name). Real face pictures were selected from a large
446 Chinese face database: the CAS-PEAL face database (Wen Gao et al., 2008). Images with
447 neutral facial expression were cropped congruently and converted to grayscale. For each
448 hierarchy structure, position 5 was always Self or Other, the face images were randomly
449 distributed to the other locations.

450 The fMRI task proceeded in 3 separate scanning sessions of 6 blocks (Self: 3 blocks,
451 Others: 3 blocks) and 150 trials each on average and took around 60 mins in total (Fig. 1).
452 Each block combined 12 learning trials followed with 13 test trials. Each learning trial
453 block included 5 superior paired trial types (red line: P1 vs P2, P2 vs P3, P1 vs P5, P2 vs
454 P5, P3 vs P5), 5 inferior paired trial types (green line: P7 vs P8, P8 vs P9, P7 vs P5, P8 vs
455 P5, P9 vs P5) and 2 intermediate paired trial types (orange line: P4 vs P5, P6 vs P5). The
456 Test trial block comprised (pink line: P1 vs P3, P2 vs P4, P3 vs P6, P1 vs P6, P4 vs P8, P6
457 vs P7, P7 vs P9, P4 vs P9, P2 vs P8, P3 vs P7, P1 vs P8, P2 vs P9, P4 vs P6). See Fig 1 for
458 a display of these pairs. The Self- and Other-orientated conditions occurred consecutively
459 with a random starting order that was indicated by a cue of text description on the screen.

460 To learn these novel diamond-shaped hierarchy structures, participants performed a three-
461 choice social hierarchy learning task. During the learning trials, they press "Left (>)",
462 "Equal (=)" or "Right (<)" within 3 s when they were shown two-paired face items on
463 the screen to indicate the relationship between the two. To confirm the reaction, the
464 pictures were highlighted with yellow or blue borders for 0.2 s, indicating whether it was a
465 Self or Other-oriented hierarchy structure respectively. The order of Self/Other trial blocks
466 and their color indications were balanced across different subjects. Then, participants
467 received a feedback screen (2 seconds) indicating Correct (+20) or Wrong (-20). In the test
468 trials, participants had to infer the relationships between the two faces that were presented
469 (pairs of non-adjacent faces from the same hierarchy) from what they had learnt before. In
470 the test phase they received no immediate feedback, however at the end of each test trial
471 block they were informed of their global score of correct responses.

472 473 **4.3 Procedure**

474 When participants arrived at the lab, they were first asked to self-administer an intranasal
475 dose of 24 IU (Oxytocin Spray— Sichuan Meike Pharmacy Co. Ltd, Sichuan, China; 3
476 puffs of 4 IU per nostril with 30 s between each puff) of either oxytocin or placebo under
477 the experimenters' supervision. Our placebo contained the same solvent (sodium chloride
478 and glycerin) but no oxytocin and was packaged in the same manufactured bottle. Then,
479 participants were required to fill out questionnaires assessing psychological measures: The
480 State-Trait Anxiety Inventory (STAI, subscales: SAI and TAI) to evaluate state and trait
481 anxiety, the Beck Depression Inventory (BDI) to assess depression, and the Positive and
482 Negative Affect Schedule (PANAS, subscales: PAS and NAS) to rate current affective
483 state.

484 Prior to the scanning session, to motivate learning of the hierarchy task, subjects were
485 given a cover story. They role-played as a candidate applying for a job at their ideal
486 company. Concurrently, they imagined another person X (a stranger) also applying for this
487 job. Subsequently they completed 10 low difficulty multiple choice questions,
488 representing personality, math and literature (e.g., general knowledge: "How do you use a
489 knife and fork?"; math tests: "According to the net of a cube below, select a valid way to
490 reshape it."). These had to be answered by subjects within 5 mins. Then, participants were
491 told that both he and the X person would be assigned to corresponding positions in two
492 different departments of the company based on their scores.

493 Once the quiz was completed, the participants received experimental instructions, that
494 they and X were employed by department A (B) and B (A) separately. As beginners, they
495 were required to learn the relationship between each person's level of competence in each
496 of the two departments, to better integrate into the organization. Instructions were also
497 included with respect to the learning and test trials in the hierarchy task. We briefly
498 repeated these instructions at the beginning of pretest program which comprised three
499 trials in the Self- and Other-orientated hierarchy conditions, to confirm they thoroughly
500 understood the task. Afterwards, 16 pictures were presented in a random order three times,
501 each for 2 seconds to reduce the potential effects of novel stimuli during the scanning
502 procedure. 30 minutes after the administration of the spray participants began to perform
503 the formal task which took about 60 minutes in the MRI scanner. When the fMRI
504 experiment finished, participants completed a self-reported questionnaire to investigate
505 their attitude towards the study, as well as the State Anxiety Inventory (STAI-SAI), the
506 Positive and Negative Affect Schedule (PANAS), Social Dominance Orientation Social

(SDO), Achievement Motivation Scale (AMS) and Iowa-Netherlands Comparison Orientation Measure (INCOM), to control the emotion and personality variables (Supplementary Table S5).

4.4 Behavioral analysis

Performance was modeled using a generalized linear mixed-effects model (GLMM) with a logit link function for the binomial (correct/ wrong) answer by the glmer function in ‘lme4’ package on R, allowing random intercepts per subjects. The fixed effects included 4 variables (Group (OXT/Placebo), Hierarchy-orientation condition (Self/Other), Status (Superior, Intermediate, Inferior), Block (1 to 9)), and their 2-way interaction factors. Non-significant interactions would be excluded from final models. For response time (RT), we used a linear mixed model (LMM) to analyze data with the lmer function in ‘lmerTest’ package on R. Follow-up tests of significant main effects or interactions were conducted using the ‘emmeans’ package. Detailed results tables for all models are reported in Supplementary files.

4.5 Computational modeling

The social hierarchy structure concerned both equal and different ranks, which makes it two dimensional and hence harder to learn than linear hierarchies. Consequently, we developed a new RL-ELO model, termed Combined RL-ELO-based associative learning models (Model 5, detailed below), enabling the model to learn hierarchical structures involving equal ranks. Because learning equal ranks may involve different strategies than learning unequal ranks, we assumed that learning equal ranks was equivalent to memorizing matching pairs. For this reason, we propose a model in which learning happens in two steps. Firstly, the Model 5 increased equality pair trial weights, when updating value processes, by judging the paired trial as equal or unequal response p_{eq} in the first step, with learning rate α_{asso} , using an associative learning model (Equation 1~2). Secondly, participants updated their representation of the structure of the hierarchy by updating the value of each item in the pair according to the past choice and reward. Each item value was evaluated within the internal hierarchy structure, with learning rate α in unequal trials, and the chosen item and learning rate α_{eq} in equal trials by the RL-ELO model (Equation 3~10). That is, the model increased (or decreased respectively) the value

of the highest (or the lowest) item in the hierarchy. If both items were equal in the hierarchy, their values became closer according to a proportion (α_{eq}) of their initial distance. The softmax choice rule (Equation 11~14) converted action values (e.g., V_L) to action probabilities (e.g., p_L). The inverse temperature β , controlled the steepness of the softmax function, which decides how decisively the response alternatives contrast with each other.

4.6 RL-ELO model combining associative and structure learning (Model 5)

Free parameters: α_{asso} = learning rate of associative learning; α = learning rate in unequal trial chosen item; α_{eq} = proportion of the distance items' value are brought closer after equal feedback; δ_1 = weight on value from associative learning; δ_2 = weight on values from global structure learning; γ = bias representing preference towards selecting the equal response; β = temperature representing the stochasticity of choices.

Associative learning (distinguish '=' and '<>' choices):

if choice at t-1 is '=', then $E_q = 1$

if choice at t-1 is either '<' or '>', then $E_q = -1$

$$p_{eq,t-1} = p_{(action_{t-1} = equal)} \quad (1)$$

$$Q_{eq,t} = Q_{eq,t-1} + \alpha_{asso} * (E_q - p_{eq,t-1}) \quad (2)$$

Structure learning (distinguish relationship between a pair of items):

if Left item is correct choice:

$$p_{win,t-1} = p_{L,t-1} \quad (3)$$

$$I_{L,t-1} = 1, I_{R,t-1} = -1 \quad (4)$$

if Right item is correct choice:

$$p_{win,t-1} = p_{R,t-1} \quad (5)$$

$$I_{R,t-1} = 1, I_{L,t-1} = -1 \quad (6)$$

Therefore, if previous response is unequal ('<' or '>'):

$$Q_{L,t} = Q_{L,t-1} + I_{L,t-1} * \alpha * (1 - p_{win,t-1}) \quad (7)$$

$$Q_{R,t} = Q_{R,t-1} + I_{R,t-1} * \alpha * (1 - p_{win,t-1}) \quad (8)$$

if previous response is equal ('='):

$$Q_{L,t} = Q_{L,t-1} + \alpha_{eq} * (Q_{R,t-1} - Q_{L,t-1}) \quad (9)$$

$$Q_{R,t} = Q_{R,t-1} - \alpha_{eq} * (Q_{L,t-1} - Q_{R,t-1}) \quad (10)$$

Probability of estimated action:

$$V_L = Q_L - Q_R \quad (11)$$

$$V_E = \delta_1 * Q_{eq} + \frac{\delta_2}{|Q_L - Q_R|} * N_{trial} + \gamma \quad (12)$$

$$V_R = Q_R - Q_L \quad (13)$$

Action policy (softmax function):

$$p(\text{choose option } i) = \frac{e^{\beta * V_i}}{e^{\beta * V_L} + e^{\beta * V_E} + e^{\beta * V_R}} \quad (14)$$

Lastly, several models were tested to update the item values in the hierarchy structure. For example, the Rescorla-Wagner (RW) model (Model 3) and the Value Transfer model (Model 4), which are known to fail in learning linear hierarchies as they associate equally with positive and negative outcomes. The classical RL-ELO model (Model 1) which functions successfully in learning linear hierarchy structures was also compared, as well as its form with two different learning rates for hierarchically superior and inferior members of the hierarchy (Model 2).

The Combined RL-ELO-based associative learning model increased equality pair trial weights when updating the value process by judging the paired trial to be equal or unequal response p_{eq} in the first step with learning rate α_{asso} , using the associative learning model (Equation 1~2); the next step evaluated each item's value within the internal hierarchy structure, with learning rate α in unequal trial chosen items and learning rate α_{eq} in equal trial chosen items, according to the RL-ELO model (Equation 3~10).

Model 1: RL-ELO model with 2 alphas

Classical RL models assume only a single learning rate α , ranging from 0 to 1. The higher α , the stronger the weighting of the prediction error (PE) for updating value. However, due to the three-level hierarchies (i.e., superior, intermediate, inferior), we developed two RL-ELO models. The first RL-ELO model with 2 alphas (Model 1), with α representing the learning rate for unequal choice $\alpha_{unequal}$, and the other is equal choice α_{equal} . The second RL-ELO model (Model 2), further subdivided the learning rate $\alpha_{unequal}$ into $\alpha_{superior}$ and $\alpha_{inferior}$.

RL-ELO model with 2 alphas is focused on the difference value between pairwise items in each trial. The implementation of this model is approximately similar to the process of Equation 3 to 12. What differs from these segments is the estimated equal action probability within Equation 12 which will be calculated as Equation 15:

$$V_E = \frac{\delta_2}{|Q_L - Q_R|} \quad (15)$$

Model 2: RL-ELO model with 3 alphas

This model assumes that the following three various hierarchies: superior, intermediate and inferior have their own learning rate. Therefore, the update value of unequal trials (Equation 7 to 8) is split, as when a previous pair is related to superior hierarchy, then conducted with $\alpha_{superior}$, corresponding to inferior hierarchy performed with $\alpha_{inferior}$.

Model 3 & 4: Rescorla-Wagner (RW) model & Value transfer model

The classical RW model is inspired by Pavlovian conditioning — animal learning from conditioned stimulus (CS) paired with an unconditioned stimulus (US). According to mechanism of RW model, the value transfer model contains another component, the accrued value θ from associative strength of the indirect (wrong) item paired with CS. While RW model set θ as zero.

if Left item is correct choice, trial outcome vector (O) & indirect item vector(W):

$$O_{L,t-1} = 1, O_{R,t-1} = -1 \quad (16)$$

$$W_{L,t-1} = 0, W_{R,t-1} = 1 \quad (17)$$

if Right item is correct choice, trial outcome vector & indirect item vector:

$$O_{L,t-1} = -1, O_{R,t-1} = 1 \quad (18)$$

$$W_{L,t-1} = 1, W_{R,t-1} = 0 \quad (19)$$

Update values of previous direct item:

$$V_{direct_{L,t-1}} = (O_{L,t-1} - V_{L,t-1}) * \alpha \quad (20)$$

$$V_{direct_{R,t-1}} = (O_{R,t-1} - V_{R,t-1}) * \alpha \quad (21)$$

Update values of previous indirect item:

$$V_{indirect_{L,t-1}} = V_{R,t-1} * W_{L,t-1} * \theta \quad (22)$$

$$V_{indirect_{R,t-1}} = V_{L,t-1} * W_{R,t-1} * \theta \quad (23)$$

Total update:

$$V_{L,t} = V_{direct_{L,t-1}} + V_{indirect_{L,t-1}} \quad (24)$$

$$V_{R,t} = V_{direct_{R,t-1}} + V_{indirect_{R,t-1}} \quad (25)$$

4.7 fMRI data acquisition and analyses

Brain images were collected at the Imaging Center of South China Normal University on a Siemens 3T Tim Trio scanner equipped with a 32-channel head-coil. Functional images were collected by using an echo-planar imaging (EPI) sequence (repetition time = 2000 ms, echo time = 30 ms; flip angle = 90°; slice thickness = 3.5 mm, field of view = 224 mm, in-plane resolution = 3 × 3 mm). In addition to functional images, a high-resolution anatomical scan was also collected (MDEFT, 1 × 1 × 1 mm resolution). Stimulations and response recordings were controlled by E-prime software on a Windows laptop located in the scanner control room. Choice responses were collected using a 4- button response pad.

The following pre-processing was applied: slice timing correction, spatial realignment, co-registered to the mean functional images, segmentation of structural T1 image, normalization motion correction, spatial smoothing using a Gaussian kernel of full-width-at-half-maximum 8.0 mm.

We ran four independent general linear models (GLMs) with a 2-way flexible factorial ANOVA, with Self- and Other-orientated hierarchy as a within subject factor and Group (Oxytocin/Placebo) as a between subject factor. In GLM1 and GLM3, onset regressor

649 began at the presentation of the 2 paired items with null duration, modulated by the
650 parametric regressor: action probability of the choice for correct responses by the
651 Combined RL-ELO-based associative learning model (Model 5). GLM1 was applied to
652 training trials and GLM3 to test trials. To improve overall model fit and account for
653 potential confounds, the design matrix included the following additional regressors which
654 were not analyzed: two regressors that modelled the onset of the highlighted response
655 screen and the onset of the feedback screen. Both were performed separately for training
656 trials and test trials. The GLM2 model employed a regressor at the onset of the feedback
657 screen with 2 s duration, modulated by two parametric regressors: an unsigned PE of
658 judging equal or unequal trial PE_{eq} , and an unsigned PE of choosing response action PE_i
659 by the winning Model 5. Parametric modulators were not orthogonalised with respect to
660 each other. The GLM4 was a basic GLM analysis without model parameters, which set
661 the regressor with whole test trial while the two items were displayed and the highlighted
662 response screen with actual duration.

663 For identification of brain (de)activation patterns we first applied whole-brain FWE-
664 correction with a cluster-wise threshold of $p < 0.05$, combined with an uncorrected voxel-
665 level threshold of $P < 0.001$. Next, referencing prior neuroimaging work on subjective
666 value of choice alternatives, we extracted BOLD activity from 10 mm radius spherical
667 ROI in the vmPFC ($x = -2, y = 46, z = -8$) and PCC ($x = -4, y = -30, z = 36$) according to a
668 meta-analysis of value representation (Bartra et al., 2013). We also added the left
669 amygdala as ROI, identified through the WFU PickAtlas 3 toolbox. The results were
670 visualized using the Mango image viewer software
671 (<http://rii.uthscsa.edu/mango/mango.html>). Brain regions were labeled according to the
672 automated anatomical labeling template via the xjView toolbox
673 (<http://www.alivelearn.net/xjview8/>). All significantly activated brain regions are reported
674 in Supplementary Table S5.
675

676 **References**

- 677 Aoki, Y., Yahata, N., Watanabe, T., Takano, Y., Kawakubo, Y., Kuwabara, H., Iwashiro, N., Natsubori, T., Inoue,
678 H., Suga, M., Takao, H., Sasaki, H., Gonoi, W., Kunimatsu, A., Kasai, K., & Yamasue, H. (2014). Oxytocin
679 improves behavioural and neural deficits in inferring others' social emotions in autism. *Brain*, *137*(11), 3073–
680 3086. <https://doi.org/10.1093/BRAIN/AWU231>
- 681 Apps, M. A. J., & Ramnani, N. (2014). The Anterior Cingulate Gyrus Signals the Net Value of Others' Rewards.
682 *Journal of Neuroscience*, *34*(18), 6190–6200. <https://doi.org/10.1523/JNEUROSCI.2701-13.2014>
- 683 Apps, M. A. J., Rushworth, M. F. S., & Chang, S. W. C. (2016). The Anterior Cingulate Gyrus and Social Cognition:
684 Tracking the Motivation of Others. *Neuron*, *90*(4), 692–707. <https://doi.org/10.1016/J.NEURON.2016.04.018>
- 685 Bang, D., Moran, R., Daw, N. D., & Fleming, S. M. (2022). Neurocomputational mechanisms of confidence in self
686 and others. *Nature Communications* *2022 13:1*, *13*(1), 1–14. <https://doi.org/10.1038/s41467-022-31674-w>
- 687 Baram, A. B., Muller, T. H., Nili, H., Garvert, M. M., & Behrens, T. E. J. (2021). Entorhinal and ventromedial
688 prefrontal cortices abstract and generalize the structure of reinforcement learning problems. *Neuron*, *109*(4),
689 713–723.e7. <https://doi.org/10.1016/j.neuron.2020.11.024>
- 690 Bartra, O., McGuire, J. T., & Kable, J. W. (2013). The valuation system: A coordinate-based meta-analysis of BOLD
691 fMRI experiments examining neural correlates of subjective value. *NeuroImage*, *76*, 412–427.
692 <https://doi.org/10.1016/J.NEUROIMAGE.2013.02.063>
- 693 Bartz, J. A., Zaki, J., Bolger, N., & Ochsner, K. N. (2011). Social effects of oxytocin in humans: context and person
694 matter. *Trends in Cognitive Sciences*, *15*(7), 301–309. <https://doi.org/10.1016/J.TICS.2011.05.002>
- 695 Behrens, T. E. J., Hunt, L. T., Woolrich, M. W., & Rushworth, M. F. S. (2008). Associative learning of social value.
696 *Nature* *2008 456:7219*, *456*(7219), 245–249. <https://doi.org/10.1038/NATURE07538>
- 697 Boorman, E. D., Sweigart, S. C., & Park, S. A. (2021). Cognitive maps and novel inferences: a flexibility hierarchy.
698 *Current Opinion in Behavioral Sciences*, *38*, 141–149. <https://doi.org/10.1016/J.COBEHA.2021.02.017>
- 699 Camille, N., Tsuchida, A., & Fellows, L. K. (2011). Double Dissociation of Stimulus-Value and Action-Value
700 Learning in Humans with Orbitofrontal or Anterior Cingulate Cortex Damage. *Journal of Neuroscience*,
701 *31*(42), 15048–15052. <https://doi.org/10.1523/JNEUROSCI.3164-11.2011>
- 702 Chang, S. W. C., Barter, J. W., Ebitz, R. B., Watson, K. K., & Platt, M. L. (2012). Inhaled oxytocin amplifies both
703 vicarious reinforcement and self reinforcement in rhesus macaques (*Macaca mulatta*). *Proceedings of the*
704 *National Academy of Sciences of the United States of America*, *109*(3), 959–964.
705 <https://doi.org/10.1073/PNAS.1114621109>
- 706 Chang, S. W. C., Fagan, N. A., Toda, K., Utevsky, A. V., Pearson, J. M., Platt, M. L., & Gazzaniga, M. S. (2015).
707 Neural mechanisms of social decision-making in the primate amygdala. *Proceedings of the National Academy*
708 *of Sciences of the United States of America*, *112*(52), 16012–16017.
- 709 Chang, S. W. C., Gariépy, J. F., & Platt, M. L. (2012). Neuronal reference frames for social decisions in primate
710 frontal cortex. *Nature Neuroscience* *2012 16:2*, *16*(2), 243–250. <https://doi.org/10.1038/NN.3287>
- 711 Chang, S. W. C., & Platt, M. L. (2013). *Oxytocin and social cognition in rhesus macaques: Implications for*
712 *understanding and treating human psychopathology*. <https://doi.org/10.1016/j.brainres.2013.11.006>

- 713 Chang, S. W. C., & Platt, M. L. (2014). Oxytocin and social cognition in rhesus macaques: Implications for
714 understanding and treating human psychopathology. *Brain Research*, 1580, 57–68.
715 <https://doi.org/10.1016/J.BRAINRES.2013.11.006>
- 716 Chang, S. W. C., Wincoff, A. A., & Platt, M. L. (2011). Vicarious reinforcement in rhesus macaques (*Macaca*
717 *mulatta*). *Frontiers in Neuroscience*, 0(MAR), 27. <https://doi.org/10.3389/FNINS.2011.00027/BIBTEX>
- 718 Chase, I. D., & Seitz, K. (2011). Self-Structuring Properties of Dominance Hierarchies: A New Perspective.
719 *Advances in Genetics*, 75, 51–81. <https://doi.org/10.1016/B978-0-12-380858-5.00001-0>
- 720 Cid-jofr, V., Moreno, M., Reyes-parada, M., & Renard, G. M. (2021). *Role of Oxytocin and Vasopressin in*
721 *Neuropsychiatric Disorders : Therapeutic Potential of Agonists and Antagonists*.
- 722 Clark-Elford, R., Nathan, P. J., Auyeung, B., Voon, V., Sule, A., Müller, U., Dudas, R., Sahakian, B. J., Phan, K. L.,
723 & Baron-Cohen, S. (2014). The effects of oxytocin on social reward learning in humans. *International Journal*
724 *of Neuropsychopharmacology*, 17(2), 199–209. <https://doi.org/10.1017/S1461145713001120>
- 725 Daunizeau, J., Adam, V., & Rigoux, L. (2014). VBA: a probabilistic treatment of nonlinear models for
726 neurobiological and behavioural data. *PLoS Computational Biology*, 10(1), e1003441.
- 727 Dayan, P. (1993). Improving Generalization for Temporal Difference Learning: The Successor Representation.
728 *Neural Computation*, 5(4), 613–624. <https://doi.org/10.1162/NECO.1993.5.4.613>
- 729 De Dreu, C. K. W. (2012). Oxytocin modulates cooperation within and competition between groups: An integrative
730 review and research agenda. *Hormones and Behavior*, 61(3), 419–428.
731 <https://doi.org/10.1016/j.yhbeh.2011.12.009>
- 732 De Dreu, C. K. W., Greer, L. L., Handgraaf, M. J. J., Shalvi, S., Van Kleef, G. A., Baas, M., Ten Velden, F. S., Van
733 Dijk, E., & Feith, S. W. W. (2010). The Neuropeptide Oxytocin Regulates Parochial Altruism in Intergroup
734 Conflict Among Humans. *Science*, 328(5984), 1408–1411. <https://doi.org/10.1126/SCIENCE.1189047>
- 735 Domes, G., Heinrichs, M., Kumbier, E., Grossmann, A., Hauenstein, K., & Herpertz, S. C. (2013). Effects of
736 intranasal oxytocin on the neural basis of face processing in autism spectrum disorder. *Biological Psychiatry*,
737 74(3), 164–171. <https://doi.org/10.1016/j.biopsych.2013.02.007>
- 738 Ebitz, R. B., Watson, K. K., & Platt, M. L. (2013). Oxytocin blunts social vigilance in the rhesus macaque.
739 *Proceedings of the National Academy of Sciences of the United States of America*, 110(28), 11630–11635.
740 <https://doi.org/10.1073/PNAS.1305230110>
- 741 Ereira, S., Hauser, T. U., Moran, R., Story, G. W., Dolan, R. J., & Kurth-Nelson, Z. (2020). Social training
742 reconfigures prediction errors to shape Self-Other boundaries. *Nature Communications* 2020 11:1, 11(1), 1–14.
743 <https://doi.org/10.1038/S41467-020-16856-8>
- 744 Everett, N. A., Turner, A. J., Costa, P. A., Baracz, S. J., & Cornish, J. L. (2020). The vagus nerve mediates the
745 suppressing effects of peripherally administered oxytocin on methamphetamine self-administration and seeking
746 in rats. *Neuropsychopharmacology* 2020 46:2, 46(2), 297–304. <https://doi.org/10.1038/S41386-020-0719-7>
- 747 Feng, C., Hackett, P. D., DeMarco, A. C., Chen, X., Stair, S., Haroon, E., Ditzen, B., Pagnoni, G., & Rilling, J. K.
748 (2015). Oxytocin and vasopressin effects on the neural response to social cooperation are modulated by sex in
749 humans. *Brain Imaging and Behavior*, 9(4), 754–764. <https://doi.org/10.1007/S11682-014-9333-9>
- 750 Feng, C., Zhou, X., Zhu, X., Zhu, R., Han, S., & Luo, Y.-J. (2020). *Effect of intranasal oxytocin administration on*
751 *self-other distinction: Modulations by psychological distance and gender*.
752 <https://doi.org/10.1016/j.psyneuen.2020.104804>

753 Ferguson, J. N., Aldag, J. M., Insel, T. R., & Young, L. J. (2001). Oxytocin in the Medial Amygdala is Essential for
754 Social Recognition in the Mouse. *Journal of Neuroscience*, *21*(20), 8278–8285.
755 <https://doi.org/10.1523/JNEUROSCI.21-20-08278.2001>

756 Ferguson, J. N., Young, L. J., Hearn, E. F., Matzuk, M. M., Insel, T. R., & Winslow, J. T. (2000). Social amnesia in
757 mice lacking the oxytocin gene. *Nature Genetics*, *25*(3), 284–288. <https://doi.org/10.1038/77040>

758 Gordon, I., Vander Wyk, B. C., Bennett, R. H., Cordeaux, C., Lucas, M. V., Eilbott, J. A., Zagoory-Sharon, O.,
759 Leckman, J. F., Feldman, R., & Pelphrey, K. A. (2013). Oxytocin enhances brain function in children with
760 autism. *Proceedings of the National Academy of Sciences of the United States of America*, *110*(52), 20953–
761 20958. <https://doi.org/10.1073/PNAS.1312857110>

762 Guastella, A. J., & Hickie, I. B. (2016). Oxytocin Treatment, Circuitry, and Autism: A Critical Review of the
763 Literature Placing Oxytocin into the Autism Context. *Biological Psychiatry*, *79*(3), 234–242.
764 <https://doi.org/10.1016/j.biopsych.2015.06.028>

765 Hadland, K. A., Rushworth, M. F. S., Gaffan, D., & Passingham, R. E. (2003). The anterior cingulate and reward-
766 guided selection of actions. *Journal of Neurophysiology*, *89*(2), 1161–1164.
767 <https://doi.org/10.1152/JN.00634.2002/ASSET/IMAGES/LARGE/9K0232906003.JPEG>

768 Hawthorn, J., Ang, V. T. Y., & Jenkins, J. S. (1985). Effects of lesions in the hypothalamic paraventricular,
769 supraoptic and suprachiasmatic nuclei on vasopressin and oxytocin in rat brain and spinal cord. *Brain*
770 *Research*, *346*(1), 51–57. [https://doi.org/10.1016/0006-8993\(85\)91093-5](https://doi.org/10.1016/0006-8993(85)91093-5)

771 Hayden, B. Y., & Platt, M. L. (2010). Neurons in Anterior Cingulate Cortex Multiplex Information about Reward and
772 Action. *Journal of Neuroscience*, *30*(9), 3339–3346. <https://doi.org/10.1523/JNEUROSCI.4874-09.2010>

773 Hu, J., Qi, S., Becker, B., Luo, L., Gao, S., Gong, Q., Hurlmann, R., & Kendrick, K. M. (2015). Oxytocin
774 selectively facilitates learning with social feedback and increases activity and functional connectivity in
775 emotional memory and reward processing regions. *Human Brain Mapping*, *36*(6), 2132–2146.
776 <https://doi.org/10.1002/HBM.22760>

777 Huber, D., Veinante, P., & Stoop, R. (2005). Vasopressin and oxytocin excite distinct neuronal populations in the
778 central amygdala. *Science*, *308*(5719), 245–248.
779 https://doi.org/10.1126/SCIENCE.1105636/SUPPL_FILE/HUBER-SOM.PDF

780 Hung, L. W., Neuner, S., Polepalli, J. S., Beier, K. T., Wright, M., Walsh, J. J., Lewis, E. M., Luo, L., Deisseroth, K.,
781 Dölen, G., & Malenka, R. C. (2017). Gating of social reward by oxytocin in the ventral tegmental area. *Science*
782 *(New York, N.Y.)*, *357*(6358), 1406–1411. <https://doi.org/10.1126/SCIENCE.AAN4994>

783 Hurlmann, R., Patin, A., Onur, O. A., Cohen, M. X., Baumgartner, T., Metzler, S., Dziobek, I., Gallinat, J., Wagner,
784 M., Maier, W., & Kendrick, K. M. (2010). Oxytocin enhances amygdala-dependent, socially reinforced
785 learning and emotional empathy in humans. *The Journal of Neuroscience: The Official Journal of the Society*
786 *for Neuroscience*, *30*(14), 4999–5007. <https://doi.org/10.1523/JNEUROSCI.5538-09.2010>

787 Ide, J. S., Nedic, S., Wong, K. F., Strey, S. L., Lawson, E. A., Dickerson, B. C., Wald, L. L., La Camera, G., &
788 Mujica-Parodi, L. R. (2018). Oxytocin attenuates trust as a subset of more general reinforcement learning, with
789 altered reward circuit functional connectivity in males. *NeuroImage*, *174*, 35–43.
790 <https://doi.org/10.1016/J.NEUROIMAGE.2018.02.035>

791 Janet, R., Ligneul, R., Losecaat-Vermeer, A. B., Philippe, R., Bellucci, G., Derrington, E., Park, S. Q., & Dreher, J.-
792 C. (2022). Regulation of social hierarchy learning by serotonin transporter availability.
793 *Neuropsychopharmacology* 2022, 1–8. <https://doi.org/10.1038/S41386-022-01378-2>

794 Jensen, G., Terrace, H. S., & Ferrera, V. P. (2019). Discovering Implied Serial Order Through Model-Free and
795 Model-Based Learning. In *Frontiers in Neuroscience* (Vol. 13). <https://doi.org/10.3389/fnins.2019.00878>

796 Jiang, Y., & Platt, M. L. (2018). Oxytocin and vasopressin flatten dominance hierarchy and enhance behavioral
797 synchrony in part via anterior cingulate cortex. *Scientific Reports*, 8(1), 8201. <https://doi.org/10.1038/s41598-018-25607-1>

799 Joiner, J., Piva, M., Turrin, C., & Chang, S. W. C. (2017). Social learning through prediction error in the brain. *Npj*
800 *Science of Learning*, 2(8). <https://doi.org/10.1038/s41539-017-0009-2>

801 Jurek, B., & Neumann, I. D. (2018). The oxytocin receptor: From intracellular signaling to behavior. *Physiological*
802 *Reviews*, 98(3), 1805–1908.
803 <https://doi.org/10.1152/PHYSREV.00031.2017/ASSET/IMAGES/LARGE/Z9J0021828400013.JPEG>

804 Kruppa, J. A., Gossen, A., Oberwelling Weiß, E., Kohls, G., Großheinrich, N., Cholemkery, H., Freitag, C. M.,
805 Karges, W., Wölflle, E., Sinzig, J., Fink, G. R., Herpertz-Dahlmann, B., Konrad, K., & Schulte-Rüther, M.
806 (2019). Neural modulation of social reinforcement learning by intranasal oxytocin in male adults with high-
807 functioning autism spectrum disorder: a randomized trial. *Neuropsychopharmacology*, 44(4), 749–756.
808 <https://doi.org/10.1038/S41386-018-0258-7>

809 Kumaran, D., Banino, A., Blundell, C., Hassabis, D., & Dayan, P. (2016). Computations Underlying Social Hierarchy
810 Learning: Distinct Neural Mechanisms for Updating and Representing Self-Relevant Information. *Neuron*,
811 92(5), 1135–1147. <https://doi.org/10.1016/j.neuron.2016.10.052>

812 Kumaran, D., Melo, H. L., & Duzel, E. (2012). The Emergence and Representation of Knowledge about Social and
813 Nonsocial Hierarchies. *Neuron*, 76(3), 653–666. <https://doi.org/10.1016/j.neuron.2012.09.035>

814 Kurth-Nelson, Z., Barnes, G., Sejdinovic, D., Dolan, R., & Dayan, P. (2015). Temporal structure in associative
815 retrieval. *Elifesciences.Org*, 4, 4919. <https://doi.org/10.7554/eLife.04919>

816 Lee, H. J., Caldwell, H. K., Macbeth, A. H., Tolu, S. G., & Young, W. S. (2008). A Conditional Knockout Mouse
817 Line of the Oxytocin Receptor. *Endocrinology*, 149(7), 3256–3263. <https://doi.org/10.1210/EN.2007-1710>

818 Lee, M. R., Shnitko, T. A., Blue, S. W., Kaucher, A. V., Winchell, A. J., Erikson, D. W., Grant, K. A., & Leggio, L.
819 (2020). Labeled oxytocin administered via the intranasal route reaches the brain in rhesus macaques. *Nature*
820 *Communications*, 11(1), 1–10.

821 Lee, W., Hiura, L. C., Yang, E., Broekman, K. A., Ophir, A. G., & Curley, J. P. (2019). Social status in mouse social
822 hierarchies is associated with variation in oxytocin and vasopressin 1a receptor densities. *Hormones and*
823 *Behavior*, 114, 104551. <https://doi.org/10.1016/J.YHBEH.2019.06.015>

824 Liao, Z., Huang, L., & Luo, S. (2020). Intranasal oxytocin decreases self-oriented learning. *Psychopharmacology*
825 2020 238:2, 238(2), 461–474. <https://doi.org/10.1007/S00213-020-05694-7>

826 Ligneul, R., Obeso, I., Ruff, C. C., & Dreher, J. C. (2016). Dynamical Representation of Dominance Relationships in
827 the Human Rostromedial Prefrontal Cortex. *Current Biology*, 26(23), 3107–3115.
828 <https://doi.org/10.1016/j.cub.2016.09.015>

- 829 MacBeth, A. H., Lee, H. J., Edds, J., & Young, W. S. (2009). Oxytocin and the oxytocin receptor underlie intrastrain,
830 but not interstrain, social recognition. *Genes, Brain and Behavior*, 8(5), 558–567.
831 <https://doi.org/10.1111/J.1601-183X.2009.00506.X>
- 832 Martins, D., Lockwood, P., Cutler, J., Moran, R., & Paloyelis, Y. (2022). Oxytocin modulates neurocomputational
833 mechanisms underlying prosocial reinforcement learning. *Progress in Neurobiology*, 213, 102253.
834 <https://doi.org/10.1016/j.pneurobio.2022.102253>
- 835 Meyer-Lindenberg, A., Domes, G., Kirsch, P., & Heinrichs, M. (2011). Oxytocin and vasopressin in the human brain:
836 social neuropeptides for translational medicine. *Nature Reviews Neuroscience* 2011 12:9, 12(9), 524–538.
837 <https://doi.org/10.1038/NRN3044>
- 838 Miller, K. J., Botvinick, M. M., & Brody, C. D. (2022). Value representations in the rodent orbitofrontal cortex drive
839 learning, not choice. *ELife*, 11. <https://doi.org/10.7554/eLife.64575>
- 840 Pessiglione, M., Seymour, B., Flandin, G., Dolan, R. J., & Frith, C. D. (2006). Dopamine-dependent prediction errors
841 underpin reward-seeking behaviour in humans. *Nature* 2006 442:7106, 442(7106), 1042–1045.
842 <https://doi.org/10.1038/NATURE05051>
- 843 Piva, M., & Chang, S. W. C. (2018). An integrated framework for the role of oxytocin in multistage social decision-
844 making. *American Journal of Primatology*, 80(10), e22735. <https://doi.org/10.1002/AJP.22735>
- 845 Piva, M., Zhang, X., Noah, J. A., Chang, S. W. C., & Hirsch, J. (2017). Distributed neural activity patterns during
846 human-to-human competition. *Frontiers in Human Neuroscience*, 11, 571.
847 <https://doi.org/10.3389/FNHUM.2017.00571/BIBTEX>
- 848 Qu, C., Ligneul, R., Van der Henst, J.-B., & Dreher, J.-C. (2017). An Integrative Interdisciplinary Perspective on
849 Social Dominance Hierarchies. *Trends in Cognitive Sciences*, 21(11), 893–908.
850 <https://doi.org/10.1016/j.tics.2017.08.004>
- 851 Raam, T., McAvoy, K. M., Besnard, A., Veenema, A., & Sahay, A. (2017). Hippocampal oxytocin receptors are
852 necessary for discrimination of social stimuli. *Nature Communications* 2017 8:1, 8(1), 1–14.
853 <https://doi.org/10.1038/S41467-017-02173-0>
- 854 Rudebeck, P. H., Saunders, R. C., Lundgren, D. A., & Murray, E. A. (2017). Specialized Representations of Value in
855 the Orbital and Ventrolateral Prefrontal Cortex: Desirability versus Availability of Outcomes. *Neuron*, 95(5),
856 1208-1220.e5. <https://doi.org/10.1016/j.neuron.2017.07.042>
- 857 Sharpe, M. J., Chang, C. Y., Liu, M. A., Batchelor, H. M., Mueller, L. E., Jones, J. L., Niv, Y., & Schoenbaum, G.
858 (2017). Dopamine transients are sufficient and necessary for acquisition of model-based associations. *Nature*
859 *Neuroscience* 2017 20:5, 20(5), 735–742. <https://doi.org/10.1038/NN.4538>
- 860 Thijssen, J. H. H., & Wiegierink, M. A. H. M. (1978). Intra- and extrahypothalamic vasopressin and oxytocin
861 pathways in the rat. *Cell and Tissue Research* 1978 192:3, 192(3), 423–435.
862 <https://doi.org/10.1007/BF00212323>
- 863 Tomova, L., Heinrichs, M., & Lamm, C. (2019). The Other and Me: Effects of oxytocin on self-other distinction.
864 *International Journal of Psychophysiology*, 136(January), 49–53.
865 <https://doi.org/10.1016/j.ijpsycho.2018.03.008>
- 866 Vasconcelos, M. (2008). Mini-review Transitive inference in non-human animals: An empirical and theoretical
867 analysis. *Behavioural Processes*, 78, 313–334. <https://doi.org/10.1016/j.beproc.2008.02.017>

- 868 Wang, D., Yan, X., Li, M., & Ma, Y. (2017). Neural substrates underlying the effects of oxytocin: A quantitative
869 meta-analysis of pharmaco-imaging studies. *Social Cognitive and Affective Neuroscience*, 12(10), 1565–1573.
870 <https://doi.org/10.1093/scan/nsx085>
- 871 Williamson, C. M., Lee, W., & Curley, J. P. (2016). Temporal dynamics of social hierarchy formation and
872 maintenance in male mice. *Animal Behaviour*, 115, 259–272.
873 <https://doi.org/10.1016/J.ANBEHAV.2016.03.004>
- 874 Wirth, S., Soumier, A., Eliava, M., Derdikman, D., Wagner, S., Grinevich, V., & Sirigu, A. (2021). Territorial
875 blueprint in the hippocampal system. *Trends in Cognitive Sciences*. <https://doi.org/10.1016/J.TICS.2021.06.005>
- 876 Wittmann, M. K., Kolling, N., Faber, N. S., Scholl, J., Nelissen, N., & Rushworth, M. F. S. (2016). Self-Other
877 Mergence in the Frontal Cortex during Cooperation and Competition. *Neuron*, 91(2), 482–493.
878 <https://doi.org/10.1016/J.NEURON.2016.06.022>
- 879 Yatawara, C. J., Einfeld, S. L., Hickie, I. B., Davenport, T. A., & Guastella, A. J. (2015). The effect of oxytocin nasal
880 spray on social interaction deficits observed in young children with autism: a randomized clinical crossover
881 trial. *Molecular Psychiatry* 2016 21:9, 21(9), 1225–1231. <https://doi.org/10.1038/MP.2015.162>
- 882 Zhao, W., Yao, S., Li, Q., Geng, Y., Ma, X., Luo, L., Xu, L., & Kendrick, K. M. (2016). Oxytocin blurs the self-other
883 distinction during trait judgments and reduces medial prefrontal cortex responses. *Human Brain Mapping*,
884 37(7), 2512–2527. <https://doi.org/10.1002/HBM.23190>
- 885 Zhuang, Q., Zhu, S., Yang, X., Zhou, X., Xu, X., Chen, Z., Lan, C., Zhao, W., Becker, B., Yao, S., & Kendrick, K.
886 M. (2021). Oxytocin-induced facilitation of learning in a probabilistic task is associated with reduced feedback-
887 and error-related negativity potentials. *Journal of Psychopharmacology (Oxford, England)*, 35(1), 40–49.
888 <https://doi.org/10.1177/0269881120972347>
- 889

890 **Acknowledgments**

891 We thank Y. Huang for the help in participant recruitment and scanning. We also thank all
892 of the participants who participated in the study.

893 **Funding:**

894 This research has benefited from the financial support of IDEXLYON from Université de
895 Lyon (project INDEPTH) within the Programme Investissements d’Avenir (ANR-16-
896 IDEX-0005), and of the LABEX CORTEX (ANR-11-LABX-0042) of Université de
897 Lyon, within the program Investissements d’Avenir (ANR-11-IDEX-007) operated by the
898 French National Research Agency, and the grant from the Agence Nationale pour la
899 Recherche to JCD (ANR-21-CE37-0032). This work was also supported by the National
900 Natural Science Foundation of China (No. 31970982 and No. 32171019). J.L was
901 supported by the China Scholarship Council.

902 **Author contributions:**

903 Conceptualization: J.L, C.Q, S.L, J.D

904 Methodology: J.L, R.P, S.L,
905 Investigation: J.L, S.L,
906 Visualization: J.L
907 Supervision: C.Q, J.D
908 Writing—original draft: J.L, R.P,
909 Writing—review & editing: J.L, E.D, B.C, J.D

910
911 **Declarations of interests:**

912 Authors declare that they have no competing interests.

913
914 **Data and materials availability:**

915 All data needed to evaluate the conclusions in the paper are present in the paper, the
916 Supplementary Materials, and the OSF repository:

917 https://osf.io/wjbpz/?view_only=d9ed0a26788b45a98e51e367059e0588

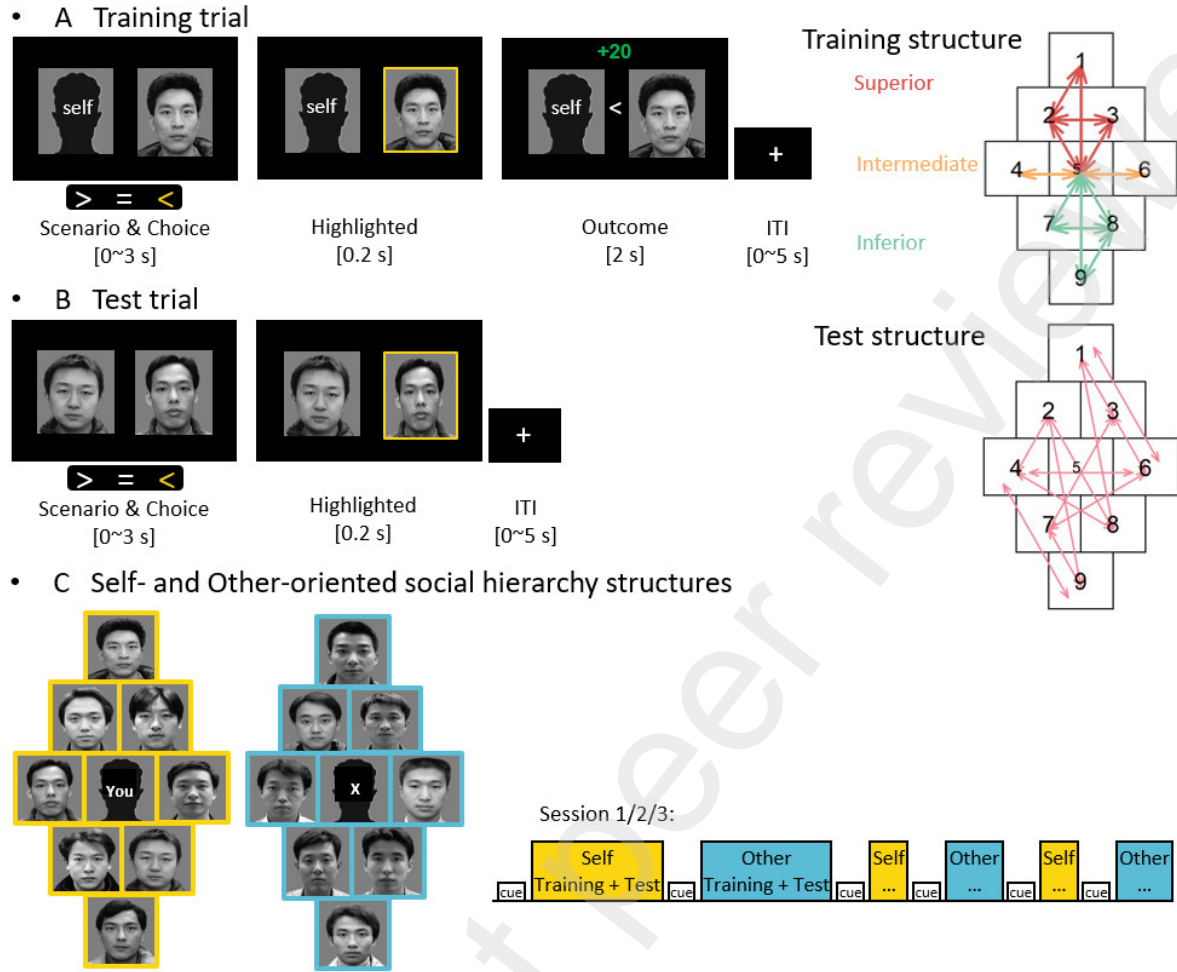
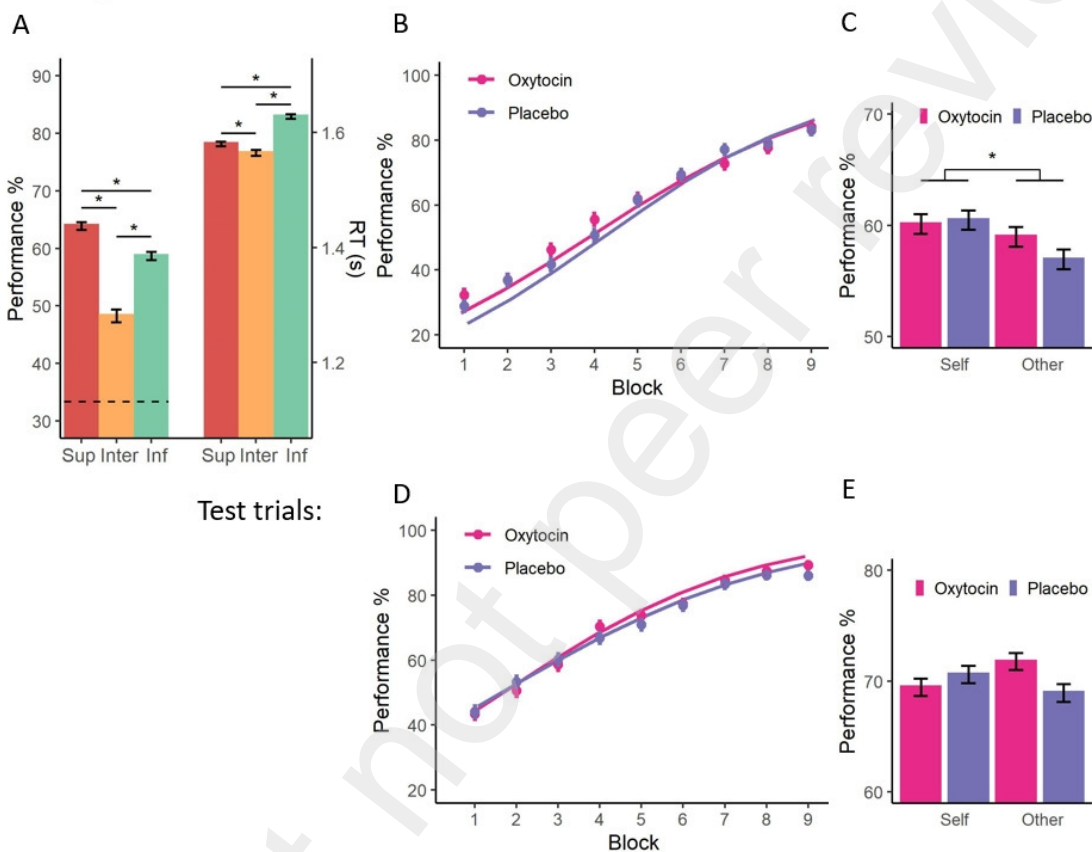


Fig. 1. Task structure. (A) On each training trial, two members of the social hierarchy were presented. Participants indicated their hierarchical relationship from the three available options: Left is superior (>), equal status (=), or right is superior (<) within 3 s. After the decision, the higher rank item's border was highlighted for 0.2 s (if “=” was pressed, both borders lighted up at the same time), and the outcome feedback was presented for 2 seconds subsequently: right (+20) or wrong (-20). Each trial finished with an ITI showing a jittered fixation (1–5 s). The right panel shows the relationships between members of the social hierarchy structure which were presented together, composing 12 training trials: 5 superior pairs (red line: P1 vs P2, P2 vs P3, P1 vs P5, P2 vs P5, P3 vs P5), 5 inferior pairs (green line: P7 vs P8, P8 vs P9, P7 vs P5, P8 vs P5, P9 vs P5) and 2 intermediate pairs (orange line: P4 vs P5, P6 vs P5). (B) Test trial blocks were presented after training trial blocks. New pairs of items, that were not in the training trial blocks were presented in a similar way, and participants attempted to infer the hierarchical relationships, however, there was no feedback. The right panel shows the social hierarchy structure contained 13 test trials (pink line: P1 vs P3, P2 vs P4, P3 vs P6, P1 vs P6, P4 vs P8, P6 vs P7, P7 vs P9, P4 vs P9, P2 vs P8, P3 vs P7, P1 vs P8, P2 vs P9, P4 vs P6). (C) The fMRI task included Self-orientated and Other-orientated social

940 hierarchy structures in which the central position (P5) is labelled as “You” or “X”
 941 respectively, along with the corresponding color (yellow or blue). However, these
 942 structures were never shown to the participants, and are presented here only to
 943 explain the experiment. The right panel illustrates one fMRI session, which
 944 comprised 3 blocks (integrated Self- and Other-orientated blocks, Self: 3 mini
 945 blocks, Other: 3 mini blocks). It was indicated in text on the cue screen whether
 946 the mini block was Self- or Other-orientated at the start of the block. (See Methods
 947 for a detailed description).
 948

Training trials:



Test trials:

949 **Fig. 2. Behavioral results.** (A) The graphs show significant main effect for hierarchy in
 950 performance accuracy and response times (RT) during training trials by GLMM1
 951 (performance) and LMM1 (RT) for superior, intermediate and inferior paired
 952 items. The dotted line indicates the performance level of random choice at 1/3. (B)
 953 Learning curve showing the mean performance of Oxytocin and Placebo groups in
 954 training trials, averaged across within-group stimuli. Participants in Placebo group
 955 were more likely learned better than Oxytocin group across time (GLMM1). (C)
 956 For illustration purposes we indicate mean performance of interaction between
 957 Groups and Hierarchy orientation, but only the Hierarchy orientation effect is
 958 significant. Performance was more likely better for the Self- than for the Other-
 959 orientated conditions (GLMM1). (D) Learning curve showing the mean
 960 performance for the Oxytocin and Placebo groups in test trials, averaging across
 961 within-group stimuli. Participants in the Oxytocin group were more likely to be
 962

perceived as learning inferences better across time than the Placebo group (GLMM2). (E) The interaction effect of Group \times Hierarchy Orientation in test trials showed that Placebo-treated participants performed better in the Self- than the Other-orientated hierarchical inference learning condition. In contrast, performance for the Other- was better than for the Self-orientated hierarchy in the Oxytocin treated group (GLMM2). Error bars correspond to SEM, lines refer to estimated performance rate.

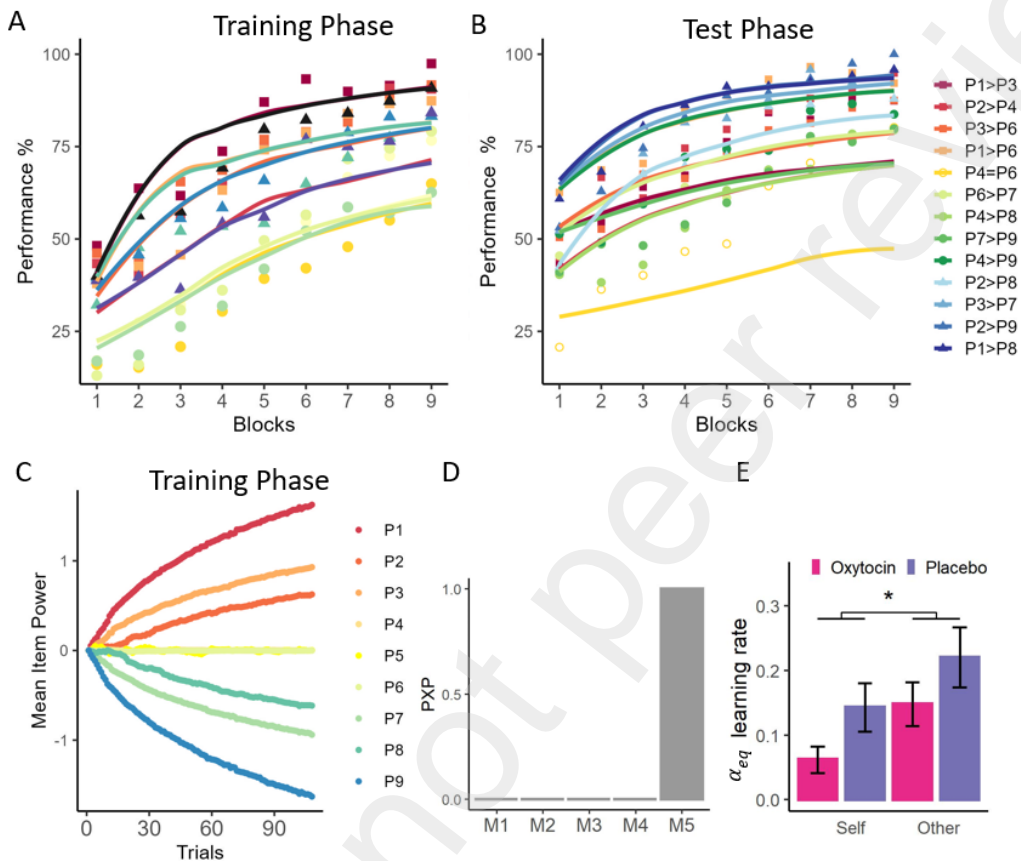
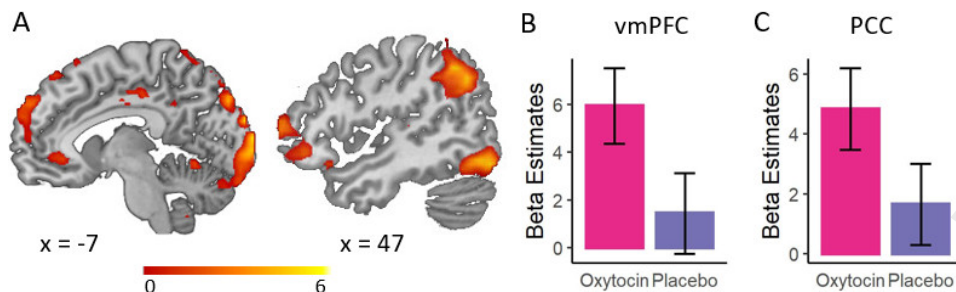


Fig. 3. Model validation on RL-ELO-based associative learning model and model comparison. (A) Learning curves, pooled over all factors estimated by the computational model with the probability of items being correct during training trials. Dots represent mean performance results of participants on that specific trial. (B) The plot shows the mean item power changed trial-by-trial, captured by the computational model, which indicates the difference between the expectation over the estimated power of the presented item. (C) Similar learning curves analysis but estimated for test trials. (D) Bayesian model selection in terms of the protected exceedance probabilities (PXP) with all subjects, which indicates that the combinatorial models based on RL-ELO and associative learning (M5) estimates decisions in hierarchy relationship better than other models: RL-ELO model with 1 alpha (M1); RL-ELO model with 3 alphas (M2); Rescorla-Wagner model (M3); Value transfer model (M4). (E) The learning rate α_{eq} of equal trials, modeled by the RL-ELO associative learning model, is higher for the Other- than Self- oriented

985 hierarchy, and marginally significantly different with respect to the treatment
986 group effect (Oxytocin or Placebo).
987



988
989 **Fig. 4. Probability to choose the correct answer in training trials.** (A) Whole-brain
990 analysis revealed a network of brain regions encoding probability to choose the
991 correct answer regardless of group (GLM 1). The regions of interest (ROI) of
992 vmPFC and PCC were defined based on a meta-analysis (see methods). (B and C)
993 Illustration of beta estimates in vmPFC and PCC and show a significant difference
994 between Oxytocin and Placebo groups. Display threshold: $P < 0.001$ uncorrected at
995 the voxel-level with $k \geq 40$. Error bars show SEM. The activation figures
996 hereinafter were made in the same way unless stated otherwise. (vmPFC =
997 ventromedial prefrontal cortex, PCC = posterior cingulate cortex).
998

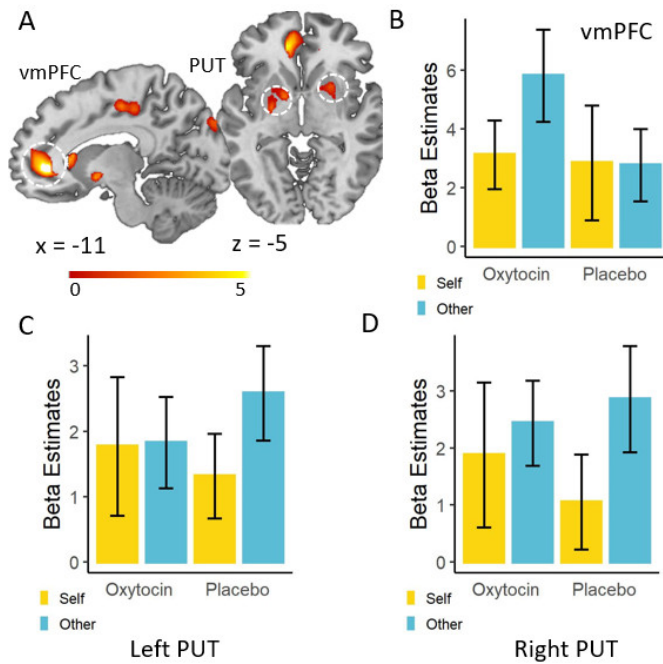
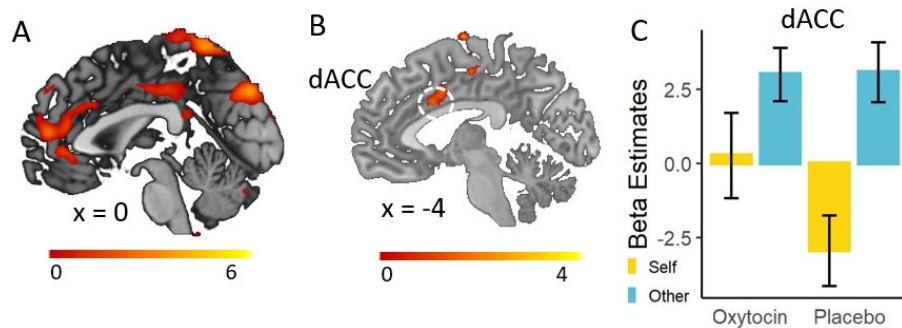
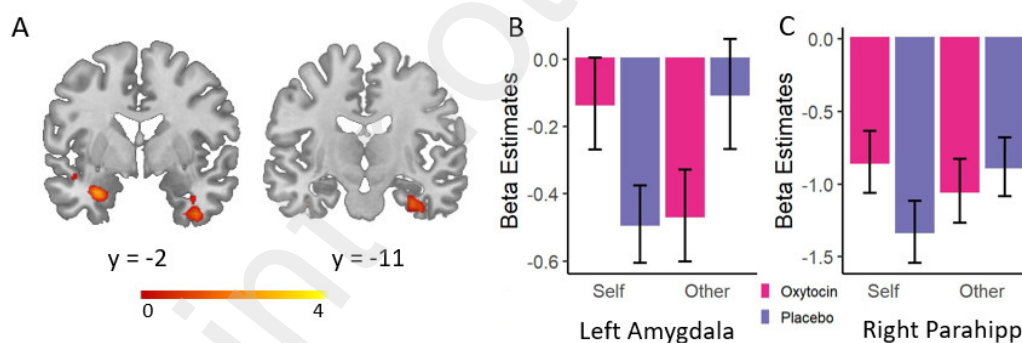


Fig. 5. Prediction error value for the winning model in training trials. (A) Whole-brain analysis revealed a network of brain regions encoding prediction error regardless of group (GLM 2). (B, C & D) Illustration of beta estimate values in vmPFC, and left and right putamen. These regions showed significant activity, but no significant differences between conditions (vmPFC: ventromedial prefrontal cortex, PUT: putamen).

1010
1011



1012 **Fig. 6. Probability to choose the correct answer of the winning model in test trials.**
1013 (A) Whole-brain analysis revealed a network of brain regions encoding the
1014 probability to choose the correct answer regardless of group by GLM 3. (B & C)
1015 Neural responses are significantly stronger to the Other- than to the Self-orientated
1016 hierarchy in the dACC (dorsal anterior cingulate cortex).
1017
1018
1019
1020
1021
1022
1023
1024
1025
1026

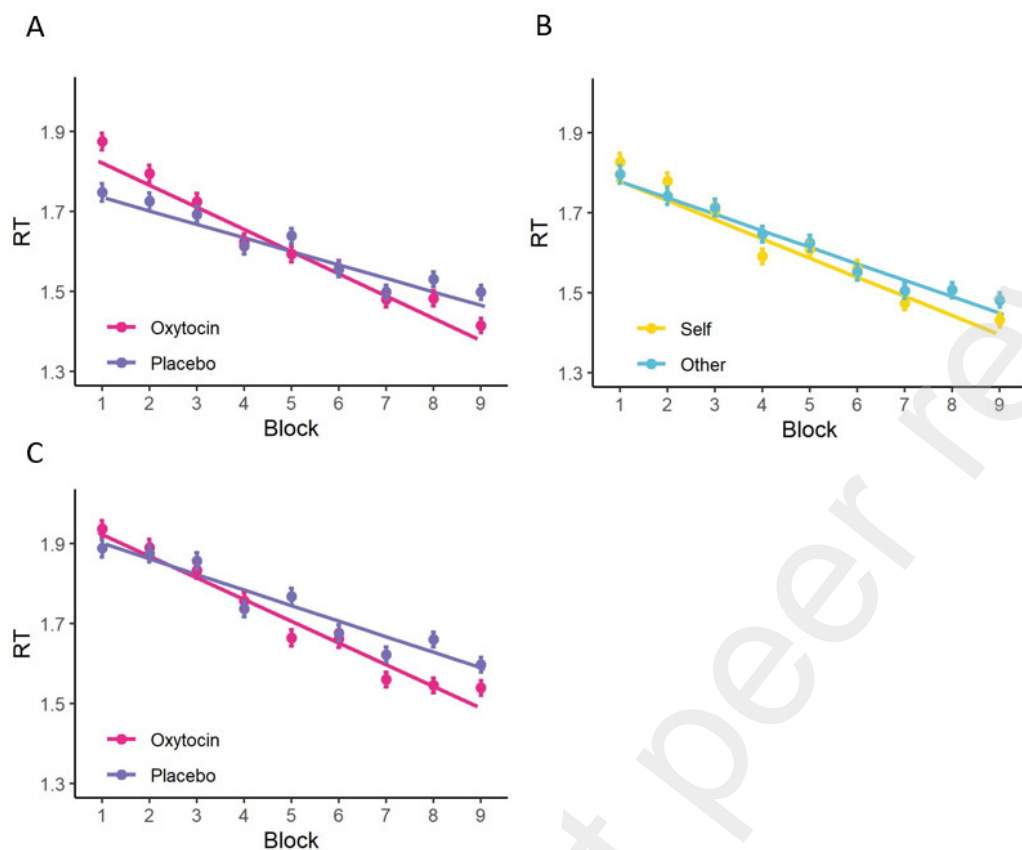


1027 **Fig. 7. Brain areas tracking the transitivity process in test trials.** (A) Interaction effect
1028 of Group \times Hierarchy Orientation in test trials showed that BOLD deactivations in
1029 the left amygdala and right inferior parahippocampal gyrus were stronger during
1030 the Self- than Other-orientated hierarchy trials in the Placebo group, while in
1031 Oxytocin group the activity was stronger for the Other- than for the Self-orientated
1032 hierarchy when tracking the transitive inference process. (B & C) Illustration of
1033 activities in amygdala and Parahippocampus showing significant differences
1034 between Oxytocin and Placebo groups.
1035
1036

1037 **Supplementary results**

1038

1039



1040

1041 **Fig. S1.**

1042 Behavior results of response time (RT).

1043 (A) RT in oxytocin group declines faster than in placebo group during learning trials.

1044 (B) RT in Self-oriented hierarchy structure declines faster than in Other-oriented hierarchy
1045 structure during learning trials.

1046 (C) RT in oxytocin group declines faster than in placebo group during test trials.

1047

1048

1049 **Table S1.**

1050 Performance results of generalized linear mixed-effects model and response time (RT) results of
 1051 linear mixed effect model in training trials.

1052

Predictor	Performance			RT		
	Odds ratios	SE	z	Beta	SE	t
(Intercept)	0.234 ***	0.022	-15.472	1.824 ***	0.03	60.595
Group (PB)	1.226	0.221	1.135	0.114	0.06	1.905
S_O (Other)	1.237 ***	0.056	4.711	0.014	0.019	0.762
Block	1.433 ***	0.014	37.503	-	-	-
				0.045 ***	0.002	27.667
Hierarchy (Superior)	3.392 ***	0.471	8.79	0.032 **	0.012	2.637
Hierarchy (Inferior)	3.156 ***	0.437	8.29	0.128 ***	0.012	10.592
Group × Block	0.966 *	0.016	-2.038	-	-	-
				0.022 ***	0.003	-6.763
S_O × Hierarchy (Superior)	0.543 ***	0.066	-5.06	0.082 **	0.024	3.401
S_O × Hierarchy (Inferior)	0.616 ***	0.074	-4.05	0.052 *	0.024	2.154
Block × Hierarchy (Superior)	0.92 **	0.023	-3.259			
Block × Hierarchy (Inferior)	0.882 ***	0.022	-5.01			
S_O × Block				-0.007 *	0.003	-2.125

1053 Notes: contrast coding of Group: 0.5 = Oxytocin, -0.5 = Placebo (reference level); contrast coding

1054 of S_O: 0.5 = Self, -0.5 = Others (reference level); contrast coding of rank: $\frac{1}{3}$ = Superior, $\frac{1}{3}$ =

1055 Intermediate (reference level), $\frac{1}{3}$ = Inferior. Block was coded as ordinal levels. Significance: * p <

1056 0.05, ** p < 0.01, *** p < 0.001.

1057

1058 **Table S2.**

1059 Performance results of generalized linear mixed-effects model and response time (RT) results of
1060 linear mixed effect model in test trials.

1061

Predictor	Performance			RT		
	Odds ratios	SE	z	Beta	SE	t
(Intercept)	0.59 ***	0.057	-5.416	1.959 ***	0.032	61.594
Group (PB)	0.881	0.172	-0.649	0.045	0.064	0.705
S_O (Other)	1.021	0.042	0.511	0.09 ***	0.019	4.821
Block	1.373 ***	0.012	36.518	-0.047 ***	0.002	-28.17
Group × Block	1.04 *	0.018	2.268	-0.015 ***	0.003	-4.672
Group × S_O	1.262 **	0.104	2.82			
S_O × Block				-0.014 ***	0.003	-4.077

1062 Notes: Reference level of Group: 0.5 = Oxytocin, -0.5 = Placebo; Reference level of S_O: 0.5 =
1063 Self, -0.5 = Others. Significance: * p < 0.05, ** p < 0.01, *** p < 0.001.

1064

1065

1066 **Table S3.**
 1067 Parameters of combined RL-ELO-based associative learning model.
 1068

Mean (SEM)		α_{asso}	α	α_{eq}	β	δ_1	δ_2	γ
Oxytocin	Self	0.55 (0.01)	0.35 (0.03)	0.06 (0.02)	0.36 (0.08)	0.59 (0.06)	0.00 (0.00)	-0.55 (0.10)
	Other	0.54 (0.01)	0.37 (0.02)	0.15 (0.03)	0.38 (0.09)	0.50 (0.08)	0.00 (0.00)	-0.57 (0.10)
Placebo	Self	0.55 (0.01)	0.41 (0.02)	0.14 (0.04)	0.24 (0.09)	0.63 (0.06)	0.00 (0.00)	-0.53 (0.08)
	Other	0.55 (0.01)	0.34 (0.02)	0.22 (0.05)	0.16 (0.11)	0.58 (0.07)	0.00 (0.00)	-0.64 (0.09)

1069 Note: SEM means standard error of the mean.

1070
 1071

1072 **Table S4.**
 1073 Brain activity related to GLMs 1-4.
 1074

Brain Region	Hemisphere	Cluster Size	T-value	MNI			BA
				x	y	z	
Regions encoding the value of chosen correct option in training phase							
(pooled all conditions; GLM1)							
Positive modulation in all subjects:							
CB/OG***	L	4311	7.34	-33	-75	-21	7/17/19
MTG/IPL***	L	1397	7	-66	-39	0	21/39/40
SFG/MFG***	L	1830	5.77	-27	27	54	8
MFG/IFG***	L	492	5.65	-39	60	-3	10/47
TG***	R	368	4.78	60	-24	-21	21/22
vmPFC**	B	88	4.58	-12	36	-9	10
MCC**	B	131	4.32	6	-30	42	31/24
Negative modulation in all subjects:							
LG*	L	62	4.34	-24	-69	-6	19
OXT > PB:							
PCC (p=0.052)	R	56	4.41	15	-24	42	31
Positive modulation in Self-orientated condition:							
CB/OG***	L	1342	6.39	-30	-75	-21	16/18
VS/Hipp***	L	186	5.67	-24	-27	9	27/13
PCUN***	B	537	5.58	3	-75	57	7/13
CB/OG***	R	287	5.1	45	-78	-18	18/19
MFG***	R	366	5.06	48	51	9	8/16
MFG***	L	161	4.96	-30	24	54	8
MTG*	L	61	4.7	-66	-39	0	21
AG***	R	181	4.69	48	-57	42	40
AG***	L	397	4.64	-42	-51	36	41
IFG*	L	71	4.46	-30	30	-15	47
Positive modulation in Other-orientated condition:							
TG***	L	236	5.23	-66	-39	0	21
LG***	R	224	4.86	9	-96	-3	17

IFG**	L	105	4.82	-39	36	-9	47
SFG***	L	251	4.47	-15	42	45	9
CB/OG***	L	206	4.35	-39	-72	-24	19/37
AG***	L	168	4.12	-57	-57	30	39/40
AG*	R	82	4.08	57	-57	24	39/40
vmPFC*	B	80	3.92	3	30	-12	11
OG/PCUN*	L	76	3.74	-12	-87	33	7
Positive modulation in Oxytocin group:							
AG/TPJ/TG***	L	1620	6.21	-54	-33	0	40/22/21
AG/TPJ/TG***	R	829	4.91	51	-30	3	40/22/21
PCC***	B	683	4.84	9	-33	51	31
MFG/IFG***	R	239	4.71	48	51	9	46/47
SFG***	L	319	4.56	-15	42	51	9
TG**	R	135	4.49	63	-9	-12	21/38
MFG/SFG**	R	122	4.47	36	39	45	8
SFG*	R	57	4.43	12	33	54	6
PCUN*	R	63	4.38	6	-96	0	17
ACC**	L	86	4.1	-9	39	0	24
vmPFC**	B	90	4	-3	57	12	10
OG*	L	79	3.72	-39	-84	-12	37
Positive modulation in Placebo group:							
CB/PCUN***	L	2156	7.66	-30	-78	-21	7/19
SFG**	L	87	4.38	-12	63	30	10
AG*	R	59	4.14	45	-63	30	40
OFC**	L	98	4.13	-39	54	-3	46
Negative modulation in Placebo group:							
IFG*	L	76	5.32	-45	3	24	9
LG*	L	80	5.04	-24	-69	-3	19
LG*	R	60	4.41	27	-51	-9	19
Regions encoding the value of prediction error in training phase							
(all conditions pooled, GLM2)							
Positive modulation in all subjects:							
vmPFC**	B	181	5.74	-12	42	0	32
Cau*	R	106	5.2	18	-6	27	

Put*	L	101	4.91	-24	-12	-3	
Put**	R	131	4.84	30	3	15	
OG*	B	124	4.51	-3	-90	33	19
Negative modulation in all subjects:							
MFG/SFG***	R	410	5.92	42	21	30	8/9
MFG/IFG***	L	458	5.82	-39	21	27	46/9
SFG/SMA***	L	253	5.76	-6	9	57	6/8
IFG/Ins*	R	94	5.33	33	21	0	47
IPL***	L	243	5.04	-36	-45	45	40
Negative modulation in Self-orientated condition:							
Thalamus*	R	117	4.46	9	-24	0	
MFG***	L	265	4.41	-39	24	27	9
MFG*	R	118	4.24	42	21	27	9
Positive modulation in Other-orientated condition:							
vmPFC*	B	108	5.15	-12	39	-3	32
Putamen*	R	93	4.11	27	9	0	
Negative modulation in Other-orientated condition:							
MFG*	R	129	4.7	42	24	27	8
MFG/IFG*	L	122	4.3	-39	21	27	
Negative modulation in Oxytocin group:							
IPL*	L	92	4.1	-36	-45	45	40
Negative modulation in Placebo group:							
MFG**	R	183	5.05	42	21	30	8
SFG/SMA***	R	260	4.9	9	24	48	6
MFG/IFG**	L	195	4.52	-42	15	30	9
IFG/Ins*	R	87	4.29	39	24	0	47
Regions encoding the value of chosen correct option in test phase							
(all conditions pooled, GLM3)							
Positive modulation in all subjects:							
IFG/MFG**	L	125	6.11	-51	30	0	47
PCUN***	R	542	5.85	9	-84	39	19

VS***	R	270	5.76	30	-21	3	13
MTG***	R	357	5.42	60	-42	-3	21
Ins**	L	108	5.27	-30	-6	3	13
SFG***	R	608	5.25	9	51	42	9
TPJ***	L	495	5.06	-54	-42	24	40
TPJ***	R	248	5.01	51	-51	30	40
IFG/MFG***	R	242	4.79	48	39	-3	46/10
CB***	L	287	4.73	-33	-75	-24	
CB/OG***	R	341	4.53	21	-93	-12	18
PCC***	B	278	4.13	12	-42	42	31
Negative modulation in all subjects:							
LG**	L	132	5.76	-15	-78	-3	18
MedFG***	B	271	5.08	-9	12	51	6
LG*	R	82	4.59	18	-75	-3	18
Other > Self:							
dACC*	R	94	4.29	15	6	45	33
PreCG*	R	78	4.21	18	-15	57	6
IPL*	R	104	3.76	57	-27	33	40
Positive modulation in Self-orientated condition:							
IFG**	L	109	5.85	-48	30	0	47
MFG*	R	99	5.18	48	39	-3	47
SFG**	R	114	4.5	9	54	42	9
AG*	R	88	4.35	48	-51	30	39
TG**	R	122	4.29	66	-33	-6	20/21
MTG**	L	107	4.17	-48	-39	0	21
SFG*	L	96	4.17	-15	27	60	9
Negative modulation in Self-orientated condition:							
Ins*	R	82	6.18	33	18	12	47
MCC/SFG***	L	383	5.38	-24	0	54	24/6
Positive modulation in Other-orientated condition:							
VS/Amy***	R	447	6.01	30	-18	6	13
OG***	R	321	5.85	36	-81	-21	19
PCUN***	R	1342	5.77	9	-84	39	19
LG***	L	254	5.57	-15	-105	-9	18

TPJ***	L	662	5.13	-51	-39	24	40/41
PoCG***	R	327	5.13	60	-24	33	2/40
TG**	R	132	4.76	63	-42	0	21
TG/OG*	L	99	4.41	-54	-57	6	37
Negative modulation in Other-orientated condition:							
LG*	L	73	4.7	-12	-75	-3	18
Positive modulation in Oxytocin group:							
TG**	L	110	5.24	-51	-36	6	22
PCUN*	R	100	4.83	6	-78	36	7
TPJ/Ins*	L	89	4.67	-54	-42	24	40/42
VS*	R	83	4.64	30	-6	6	
PCC***	B	321	4.45	3	-33	33	31
Positive modulation in Placebo group:							
TG**	R	170	4.96	63	-42	-3	21
SFG**	R	171	4.84	12	54	42	9
OG***	R	246	4.79	15	-87	36	19
OG***	L	314	4.63	-42	-84	-12	37
ACC**	B	106	4.2	3	36	-24	11
CB*	R	104	4.06	42	-75	-24	
Negative modulation in Placebo group:							
LG*	L	87	5.39	-15	-75	-3	18
Others - Self in Placebo group:							
SFG/PreCG***	B	436	4.62	6	-3	78	6/31
LG/OG*	R	84	4.29	24	-96	-9	18
CB*	L	73	4.26	-27	-81	-39	
Regions encoding the value of inferring social hierarchy in test phase (GLM4)							
Oxytocin_(Self – Other) > Placebo_(Self – Other):							
ITG**	L	131	4.27	30	12	-30	38

1075

1076

1077

Note: Regions shown here met the uncorrected voxel-level threshold of $p < 0.001$ with $k = 40$.

With the above uncorrected threshold as the cluster-defining threshold, clusters met the Family-

1078 Wise Error corrected cluster-level (cl-FWE) threshold were marked: * $p < 0.05$, ** $p < 0.01$, *** p
1079 < 0.001 .

1080 Coordinates shown here were based on Montreal Neurological Institute (MNI) coordinate system.
1081 Abbreviations: B: bilateral, L: left, R: right, BA: Brodmann Area; ACC: anterior cingulate cortex,
1082 AG: angular gyrus, Amy: amygdala, Cau: caudate, CB: cerebellum, dACC: dorsal anterior
1083 cingulate cortex, FG: fusiform gyrus, IFG: inferior frontal gyrus, Ins: insula, IPL: inferior parietal
1084 lobule, ITG: inferior temporal gyrus, LG: lingual gyrus, MCC: middle cingulate cortex, MedFG:
1085 medial frontal gyrus, MFG: middle frontal gyrus, ,MTG: middle temporal gyrus, OFC:
1086 orbitofrontal cortex, OG: occipital gyrus, PCC: posterior cingulate cortex, PCUN: precuneus,
1087 PoCG: post-central gyrus, PreCG: precentral gyrus, Put: putamen, SFG: superior frontal gyrus,
1088 SmG: supramarginal gyrus, SMA: supplementary motor area, TG: temporal gyrus, TPJ: temporal
1089 parietal junction, vmPFC: ventromedial prefrontal cortex, VS: ventral striatum.

1090

1091

1092

1093 **Table S5.**

1094 Various scales' scores on Pre - & Post - scanning task.

Scales	Oxytocin Mean	Placebo Mean	t	p
<i>Before the fMRI task</i>				
BDI	29.48 (6.07)	29.62 (7.30)	-0.078	0.938
STAI	77.62 (13.77)	75.55 (16.82)	0.513	0.61
STAI_SAI	36.38 (7.22)	34.76 (9.37)	0.738	0.464
STAI_TAI	41.24 (7.98)	40.79 (8.78)	0.204	0.839
PANAS	52.83 (7.47)	50.21 (9.26)	1.186	0.241
PANAS_PAS	32.97 (5.52)	30.90 (5.77)	1.396	0.168
PANAS_NAS	19.86 (5.41)	19.31 (7.52)	0.321	0.75
<i>After the fMRI task</i>				
STAI_SAI	35.97 (9.45)	33.28 (8.77)	1.124	0.266
PANAS	49.24 (9.07)	44.69 (9.27)	1.89	0.064
PANAS_PAS	31.76 (7.77)	29.10 (7.53)	1.321	0.192
PANAS_NAS	17.48 (5.51)	15.59 (6.27)	1.224	0.226
SDO	3.48 (1.58)	3.60 (1.79)	-1.053	0.292
SDO_GBD	3.85 (1.66)	4.22 (1.74)	-2.298	0.022 *
SDO_OEQ	3.11 (1.40)	2.99 (1.62)	0.89	0.374
INCOM	38.03 (-4.34)	38.31 (-5.53)	-0.211	0.833
INCOM_Abilities	21.03 (-2.74)	20.45 (-2.8)	0.805	0.424
INCOM_Opinions	17 (-2.24)	17.86 (-3.44)	-1.131	0.264
AMS	5.9 (17.07)	2.79 (12.01)	0.801	0.427

1095

1096

1097 **Table S6.**
 1098 Post-experimental questionnaire.

Questions	Oxytocin Mean (SD)	Placebo Mean (SD)
Please rate other's willingness to partner with someone in another Department (from your perspective) *	0.43 (1.65)	0.33 (1.78)
Please rate your willingness to partner with someone in another Department	0.48 (1.76)	0.43 (1.86)
Please rate perceived social distance with each colleague in your company	47.59 (43.71)	44.44 (25.30)
Guess whether you received oxytocin ① or placebo ②	1.38 (0.49)	1.48 (0.51)
Do the characters in your department match the ones you imagine?	2.07 (0.70)	2.10 (0.77)
Do the characters in other's department match the ones you imagine?	1.93 (0.65)	1.97 (0.68)
How would you grade your relationship with those at the top of your department?	4.24 (0.64)	4.31 (0.60)
How would you grade your relationship with those at the top of the other's department?	4.14 (0.95)	4.17 (0.80)
How would you grade your relationship with those at the lowest level of your department?	1.76 (0.91)	1.38 (0.68)
How would you grade your relationship with those at the lowest level of the other's department?	1.62 (0.82)	1.41 (0.68)
How satisfied do you feel intuitively about your company?	3.31 (0.93)	3.24 (0.83)

1099
 1100
 1101

1102 **Table S7.**

1103 Model parametric in RL-Elo associative learning model using repeated- measures ANOVAs.

Parametric	Factor	$F_{(1,56)}$	p	η^2
α_{asso}	Group	0.25	0.62	0.00293
α_{asso}	S_O	0.00	0.95	0.00003
α_{asso}	Group×S_O	0.13	0.72	0.00085
α_{eq}	Group	3.53	0.07	0.03946
α_{eq}	S_O	7.42	0.01	0.04412
α_{eq}	Group×S_O	0.02	0.88	0.00013
α	Group	0.30	0.58	0.00341
α	S_O	1.69	0.20	0.01093
α	Group×S_O	4.34	0.04	0.02766
β	Group	2.31	0.13	0.03025
β	S_O	0.21	0.65	0.00091
β	Group×S_O	0.69	0.41	0.00301
δ_1	Group	0.49	0.49	0.00592
δ_1	S_O	1.59	0.21	0.00900
δ_1	Group×S_O	0.08	0.78	0.00047
δ_2	Group	3.01	0.09	0.02588
δ_2	S_O	1.13	0.29	0.01015
δ_2	Group×S_O	0.03	0.86	0.00030
γ	Group	0.05	0.82	0.00075
γ	S_O	1.06	0.31	0.00428
γ	Group×S_O	0.65	0.42	0.00262

1104 Note: We examined differences between Self/Other hierarchy conditions (S_O) in the model
1105 parametric at the group level using repeated-measures ANOVAs.

1 **Oxytocin modulates the neurocomputational mechanisms**
2 **engaged in learning social hierarchy**

3
4 **Authors**

5 Jiawei Liu^{1,2,3†}, Chen Qu^{3†}, Rémi Phillippe^{1,2}, Siying Li^{3,4}, Edmund Derrington^{1,2}, Brice
6 Corgnet⁵, Jean-Claude Dreher^{1,2*}

7 ¹ Laboratory of Neuroeconomics, Institut des Sciences Cognitives Marc Jeannerod,
8 CNRS, Lyon, France.

9 ² Université Claude Bernard Lyon 1, Lyon, France.

10 ³ Key Laboratory of Brain, Cognition and Education Sciences, Ministry of Education,
11 China; School of Psychology, Center for Studies of Psychological Application,
12 and Guangdong Key Laboratory of Mental Health and Cognitive Science, South China
13 Normal University, China.

14 ⁴ Faculty of Education, Northeast Normal University, Changchun, China.

15 ⁵ EM Lyon Business School, and CNRS, GATE Lab, UMR 5824, Ecully, 69130, France.

16 † These authors contributed equally to this work.

17
18 * Lead contact, Correspondence: dreherjeanclaude@gmail.com
19
20